DEGRADABLE HYDROGELS FOR LOCAL DRUG DELIVERY

by
Bianka Golba
B.S., Chemistry, Boğaziçi University, 2017

Submitted to the Institute for Graduate Studies in
Science and Engineering in partial fulfillment of
the requirements for the degree of
Master of Science

Graduate Program in Chemistry
Boğaziçi University
2019

DEGRADABLE HYDROGELS FOR LOCAL DRUG DELIVERY

APPROVED BY:

Prof. Amitav Sanyal ……

(Thesis Supervisor)

Prof. Rana Sanyal ……

Assist. Prof. Özgül Gök ……

DATE OF APPROVAL: 29.05.2019

ACKNOWLEDGEMENTS

First of all, I would like to thank my thesis supervisor Prof. Amitav Sanyal for accepting me as his master student, as well as for his guidance, training, support and many research opportunities he gave since my undergraduate years until the end of my master studies. I feel very lucky to be able to work on several major and minor research projects under his mentorship and discover my scientific interests for the following journeys.

I would also like to express my gratitudes to Prof. Rana Sanyal for accepting me to her lab at first place, encouraging and galvanizing me into doing research since my undergraduate years. I would like to thank for the huge support and chances she gave me in every aspect of my academic life.

I am also very grateful to my jury member Asst. Prof. Özgül Gök for reviewing and helping me improve my thesis.

Additionally, I would like to thank to my family for their immense support, encouragement and patience all the time.

I would like to thank Burcu Sümer Bolu for kindling my interest in lab work at the beginning of my research journey, for her patience and friendship. I would also like to thank my labmates for their friendship and support.

Finally, I would like to thank The Scientific and Technological Research Council of Turkey (TÜBİTAK) for supporting me through BIDEB-2210E scholarship during my master studies.

ABSTRACT

DEGRADABLE HYDROGELS FOR LOCAL DRUG DELIVERY

Hydrogels are widely utilized in biomedical applications owing to their controllable physical and chemical properties. Their physical strength, elasticity, porosity, water uptake capacity, degradability and biocompatibility can be tuned according to the application of interest. Tunability of the final properties makes them useful constructs for cancer related applications such as tumor models, diagnostic systems and smart drug delivery platforms.

The aim of this thesis was to obtain stimuli-responsive degradable hydrogels for local drug delivery in cancer therapy. For this purpose, a functionalizable copolymer, poly(PEGMEMA-*co*-SCEDEMA), was synthesized via RAFT polymerization. Hydrogel formation was achieved by crosslinking this copolymer with PEG-diamine through a disulfide-based redox and carbamate-based acid sensitive linker. In order to show the tunability of physical properties, PEG-based crosslinker length was chosen as variable. Hydrogels were shown to have lower physical strength but greater porosity and water uptake with increasing crosslinker length. This also had a considerable impact on degradation rate which was expected to influence drug release behavior. To examine this, DOX was chemically bound to hydrogels via the same dual stimuli responsive, disulfide and carbamate bearing side chain which was also utilized for crosslinking as well. Dual-responsive hydrogels were desired in order to introduce a tumor environment sensitive character into hydrogels. This responsivity was designed considering the slightly acidic and reducing conditions of tumor environment. Drug release was investigated under physiological (pH = 7.4), acidic (pH =5.5) and GSH containing acidic environment. As expected, sustainable release of DOX was achieved reaching around 80% cumulative release under GSH containing acidic conditions accompanied by the total degradation of hydrogel construct.

ÖZET

LOKAL İLAÇ SALIMI İÇİN BOZUNABİLİR HİDROJELLER

Hidrojeller kontol edilebilir fiziksel ve kimyasal özellikleri sebebiyle biyomedikal uygulamalarda sıklıkla kullanılmaktadırlar. Hidrojellerin fiziksel dayanıklılık, esneklik, gözeneklilik, su tutma kapasitesi, bozunabilirlik ve biyouyumluluk gibi birçok özelliği arzu edlilen uygulama alanına göre ayarlanabilmektedir. Bu özelliklerin kontrol edilebilir olması sayesinde kanser ile ilgili tümör modelleri, tanı sistemleri ve akıllı ilaç salım platformları gibi alanlarda sıkça kullanılmaktadırlar.

Bu tez çalışmasının hedefi kanser tedavisi için lokal ilaç salımı yapabilen çeşitli uyarıcıların tetiklemesiyle bozunabilir hidrojeller elde etmektir. Bu amaçla fonksiyonel hale getirilebilir bir polimer olan poly(PEGMEMA-*co*-SCEDEMA), RAFT polimerizasyonu kullanılarak sentezlenmiştir. Hidrojeller bu polimerin PEG-diamin yardımıyla redoks ve aside duyarlı olacak şekilde çapraz bağlanması sonucu elde edilmiştir. Hidrojellerin fiziksel özelliklerinin kontrol edilebilirliğini göstermek için çapraz bağlayıcı uzunluğu bir değişken olarak belirlenmiştir. Kullanılan çapraz bağlayıcının uzunluğu arttıkça hidrojellerin fiziksel dayanıklılıklarının azaldığı fakat gözenekli yapılarının arttığı gösterilmiştir. Aynı zamanda bunun ilaç salımı üzerinde tesiri olması öngörülen bozunurluk hızını göz ardı edilemeyecek şekilde etkilediği gözlenmiştir. Bu etkiyi analiz etmek amacıyla DOX ilacı hidrojellere kimyasal olarak polimer üzerindeki bisulfit ve karbamat bulunduran, iki farklı stimuliyle kırılabilen yan dallardan çapraz bağlayıcı ile aynı mekanizmayı kullanarak bağlanmıştır. İki farklı uyarana cevap veren hidrojel tasarlamadaki amaç tümör dokusundaki uyaranlara karşı hassas bir yapı oluşturmaktır. Bu hassasiyet, tümör dokusunun hafif asidik ve indirgeyici ortamı göz önünde bulundurularak tasarlanmıştır. İlaç salımı fizyolojik (pH = 7.4), asidik (pH =5.5) ve GSH bulunduran asidik koşullarda incelenmiştir. Öngörüldüğü üzere GSH bulunduran fizyolojik koşullarda sürdürülebilir bir şekilde %80 üzeri toplam DOX salımına ulaşılmış ve aynı zamanda hidrojellerin bozunduğu gözlenmiştir.

TABLE OF CONTENTS

LIST OF FIGURES

LIST OF TABLES

LIST OF ACRONYMS/ABBREVIATIONS

3D	3 dimensional
ACN	Acetonitrile
AIBN	2,2′-azobis(2-methylpropionitrile)
ATRP	Atom transfer radical polymerization
BTZ	Bortezomib
$CDCl_3$	Deuterated Chloroform
CH_2Cl_2	Dichloromethane
CRP	Controlled radical polymerization
CTA	Chain Transfer Agent
DMAc	Dimethylacetamide
DMSO	Dimethyl Sulfoxide
DOX	Doxorubicin
DSC	N,N′-Disuccinimidyl carbonate
DTT	Dithiothreitol
FRP	Free radical polymerization
FTIR	Fourrier Transform Infrared Spectroscopy
G’	Storage Modulus
G’’	Loss Modulus
GPC	Gel Permeation Chromatography
GSH	Glutathione
HG	Hydrogel
HPLC	High Performance Liquid Chromatpgraphy
kDa	Kilo Dalton

LCMS	Liquid Chromatography Mass Spectrometry
LVE	Linear Viscoelastic
MMP	Matrix metalloproteinase
M_n	Number Average Molecular Weight
M_w	Weight Average Molecular Weight
MsCl	Methanesulfonyl chloride
NaOAc	Sodium Acetate
NHS	N-Hydroxysuccinimide
NMR	Nuclear Magnetic Resonance
PAA	Poly(acrylic acid)
PBS	Phosphate Buffer Saline
PDEAEM	Poly(N,N′-diethylaminoethyl methacrylate)
PDI	Polydispersity index
PEG	Poly(ethylene glycol)
PEGDMA	Poly(ethylene glycol) dimethacrylate
PEGMEMA	Poly(ethylene glycol) methyl ether methacrylate
PFPA	Pentafluorophenylacrylate
PGA	Poly(glycolic acid)
PLA	Poly(lactic acid)
PMMA	Poly(methyl methacrylate)
PVA	Poly(vinyl alcohol)
RAFT	Reversible Addition Fragmentation Polymerization
RGD	Arginylglycylaspartic Acid
rt	Room Temperature
SEM	Scanning Electron Microscopy

TEA	Triethylamine
THF	Tetrahydrofuran
TME	Tumor microenvironment
UV	Ultraviolet
Vis	Visible

1. INTRODUCTION

1.1. Hydrogels

Hydrogels are polymeric 3D networks which are hydrophilic in nature. These networks are able to absorb large amounts of water with respect to their dry weight. They are frequently used in biomedical and pharmaceutical applications such as biosenors, artificial organs and drug delivery agents because of their similarity to natural tissue [1]. Hydrogels are considered to be ‘‘physical’’ or ‘‘reversible’’ if polymer chains are held together through molecular entanglements or non-covalent forces such as hydrophobic interactions, hydrogen bonding and ionic forces. In this case, reversibility comes from the disintegration of 3D network in the presence of an external environment preventing secondary interactions. On the other hand, hydrogels are considered to be ‘‘chemical’’ or ‘‘permanent’’ whenever they are crosslinked through covalent bonds in an irreversible manner [2].

Synthesis of chemical hydrogels can be performed in two ways. First, hydrogels can be obtained by 3D polymerization which is achieved by co-polymerization of mono- and poly-funtional hydrophilic monomers in the presence of initiators (Figure 1.1a). However, hydrogels which are prepared using 3D polymerization method often bear residual unreacted monomers, crosslinkers and initiators which are difficult to eliminate post-hydrogelation [3]. Since small reactive molecules are reported to be internalized more easily by cells and cause toxicity in biological environment, several strategies are developed to prevent generation of unreacted monomers and byproducts in 3D polymerization [4]. For instance, macromolecular monomers having a molecular weight range between 2-40 kDa are known to be less toxic and can be used instead of small reactive monomers. Another strategy is deactivation of residual reactive monomers post-polymerization using methods such as irradiation [5]. In order to minimize the concern for toxicity, chemical hydrogels can be fabricated by a second method which is crosslinking of already synthesized water soluble polymers via heat, light or by employing a crosslinking agent (Figure 1.1b). Since this

second method excludes utilization of reactive monomer species, purification step is not a major concern for toxicity which is advantageous for biological applications [3].

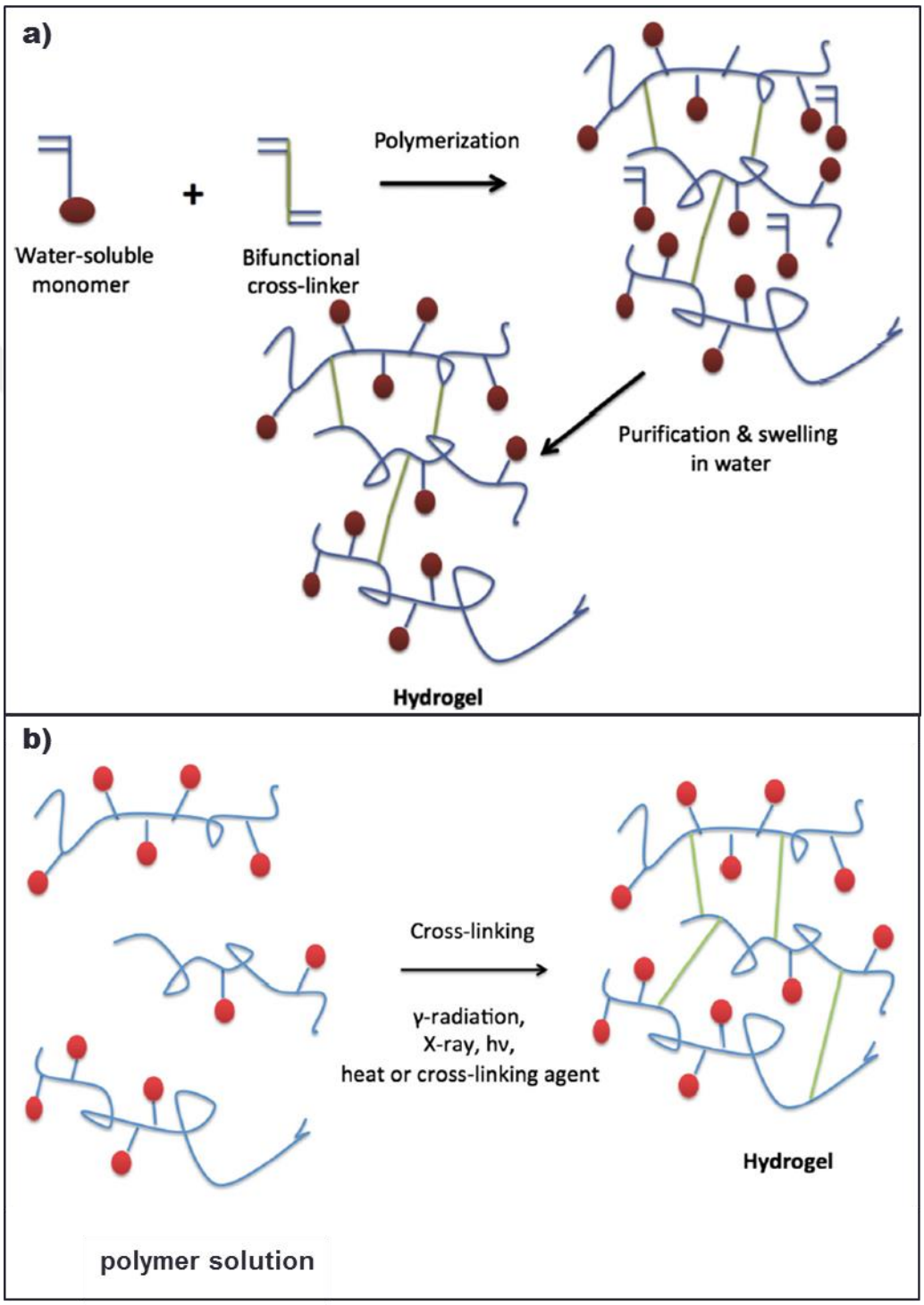

Figure 1.1 Synthesis of chemical hydrogels via a) 3D polymerization, b) crosslinking of water soluble polymers [3].

1.2. Synthesis of Hydrogels from Hydrophilic Polymers

The polymer used for hydrogel synthesis needs to be chosen attentively because it largely determines the physical and chemical properties of the final 3D network[6]. These polymers can be basically classified as natural and/or synthetic polymers. Each of these types of polymers come along with their specific advantages and drawbacks.

To begin with the natural polymers, hydrogels derived from polysaccharides and proteins are widely used for biomedical applications due to their excellent biocompatibility, biodegradability and low toxicity of by-products generated upon degradation [7]. Chitosan, cellulose and hyaluronic acid are some of the polysaccharides used for hydrogel synthesis while silk and collagen can be mentioned as protein-based biopolymer alternatives [8]. These biopolymers are profited in a wide range of biomedical applications including drug delivery and tissue engineering. For instance, Kim and Shin and coworkers utilized biodegradable chitosan hydrogels for local delivery of an anticancer drug and showed that these hydrogels inhibit tumor growth when they are combined with immunotherapy [9].

However, natural polymers often have limitations in solubility and processability in terms of industrial applications [10]. Thus, hydrogels made from synthetic polymers have become a topic of interest owing to the variability of polymeric structures according to specific needs of applications. Synthetic approach makes the hydrogel tunable because physical and chemical properties such as degradation rate, hydrophilicity, water uptake, biocompatibility and mechanical strength can be engineered by changing the chemical composition of the starting polymer or the crosslinking agent [11]. Thus, hydrogels made from synthetic polymers such as poly(vinyl alcohol) (PVA), poly(acrylic acid) (PAA) poly(lactic acid) (PLA), poly(glycolic acid) (PGA) and their copolymers are largely used for tissue engineering applications in literature [12].

Moreover, hydrogel networks synthesized via controlled radical polymerization (CRP) techniques are also in the scope of researchers [13]. For instance, CRP techniques such as reversible addition fragmentation chain transfer (RAFT) polymerization and atom transfer radical polymerization (ATRP) are reported to yield a more homogenous polymer network compared to free radical polymerization (FRP) [14]. Another advantage of CRP is that the

ratio of monomers can be tuned as desired for the application of interest. A model study was reported by Gooding and coworkers who showed that the mechanical properties of hydrogels can be tuned simply by varying the ratio of repeating units in the polymer while keeping the molecular weight same [15]. In this study, poly(ethylene glycol) methyl ether acrylate (PEGMEMA) was copolymerized with pentafluorophenylacrylate (PFPA) via RAFT polymerization (Figure 1.2). The resulting copolymer was then functionalized with norbornene groups and crosslinked via thiol-ene chemistry. Not only the crosslinking but also the functionalization with biomolecules was carried out through norbornene units. Thus, tailoring of functional repeating units via RAFT polymerization had an impact on both physical properties of hydrogels and their functionalization highlighting a significant control over the resulting material.

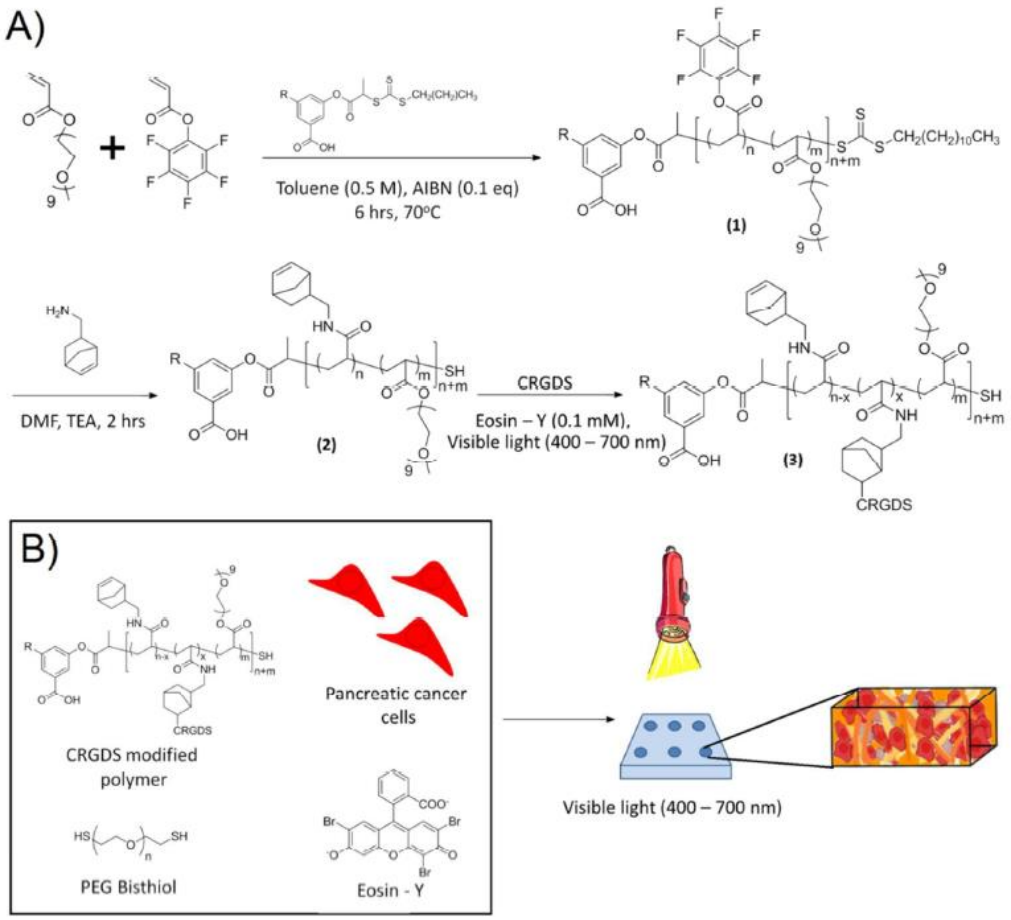

Figure 1.2. Synthesis of copolymer with norbornene functional units *via* RAFT [15].

1.3. Hydrogels in Cancer Therapy

Hydrogels are prominent in many biomedical applications such as drug delivery, tissue engineering and wound healing due to their biocompatibility, controllable degradability and mechanical properties [16]. Owing to these exceptional properties, they are also exploited in many applications related to cancer (Figure 1.3) which is one of the major diseases worldwide. According to American Cancer Society's statistics, the estimated number of new incidents is 1,762,450 while the estimated number of deaths due to cancer is reported as 606,880 for 2019, only in United States [17].

Although it became a severe threat and causes death of thousands of people every year, mechanisms underlying cancer cells' proliferation and negative responses to treatment are not totally understood yet [18]. Thus, new platforms are required for in depth investigation of cancer cell behavior. Recently, many researchers profited from hydrogels as porous 3D networks for growth and proliferation of tumor cells [19–21]. For instance, Zorlutuna and coworkers developed PEG and gelatin-based 3D hydrogel networks with tunable stiffness [21]. This 3D platform which was mimicking complex tumor microenvironment (TME) was utilized to investigate cell growth, migration and metabolic activity of human breast cancer spheroids *in vitro*. In addition, this tumor mimicking network was suggested as a drug screening platform for breast cancer studies.

Besides 3D tumor mimicking models, hydrogels are utilized for many different purposes such as temporary spacers, microwell platforms, implants, diagnostic chips and drug delivery vehicles in diagnosis and treatment of cancer [18].

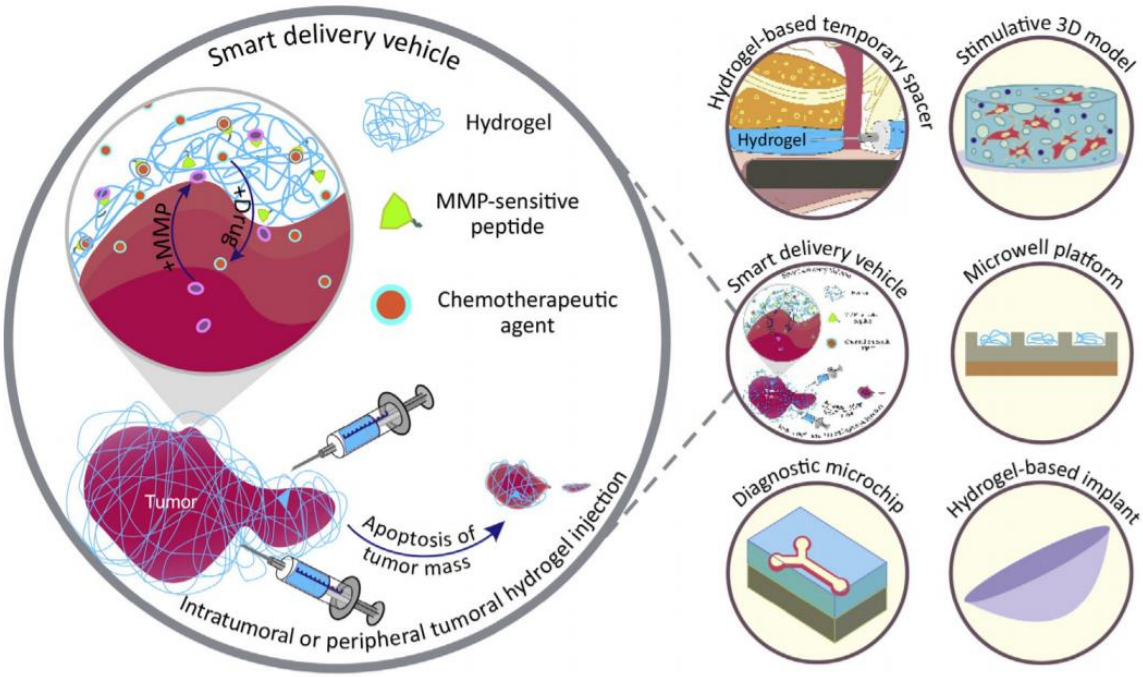

Figure 1.3. Applications of hydrogels in cancer therapy [18].

Drug delivery is a widely studied topic among those due to considerable advantages of hydrogels compared to nanomaterials when local delivery is concerned. Although nanomaterials can be equipped with targeting skills and factors reducing burst release and renal elimination [22], their localization efficiency largely depends on vascular permeability of complex tumor tissue [18]. Especially in such cases, hydrogels are good candidates for localized cancer therapy thanks to their adjustable physical properties and degradation behavior [23]. They are shown to enable local and sustained release of drug molecules, prolong their retention period while avoiding degradation of less stable ones and hereby increase the efficacy when they are administered into the tumor tissue [23,24]. Not only drugs, but also biomolecules such as siRNA which are known to have low blood stability can be locally administered via hydrogels which can release their content in a sustained manner [25]. Thus, chemotherapeutic content of hydrogels is not limited to drug molecules.

In addition, there are several ways to control the local drug delivery trends of hydrogels. For instance, depending on the desired speed of release, the drug can be loaded physically [26] or can be conjugated chemically [27] to the hydrogel. Another factor affecting drug release rate is the degradability of 3D network. Hydrogels can be designed to

degrade and/or release their content through external or internal stimuli triggers [28]. This type of design provides a control over the release of chemotherapeutic agent as well as clearing the construct from the body without further interference once its mission is complete.

1.4. Stimuli Responsive Smart Hydrogels for Local Drug Delivery

Hydrogels can be designed as smart drug delivery networks for local delivery in cancer therapy. They can be programmed to release their drug content only in the presence of a stimuli in a sustained or on-demand manner [28]. These triggers include change in intrinsic factors such as pH or temperature, presence of reducing media and molecular recognition or extrinsic factors such as electromagnetic radiation [7].

However, the way the hydrogel construct responds to these stimuli determines the mechanism of drug release. In turn, the extent and kinetics of drug release largely depends on this mechanism. An important parameter here is the ratio between mesh size and drug size mostly when a non-covalent drug loading is considered (Figure 1.4). This relation can be summarized as following, whenever the mesh size is much larger than the drug size, the drug is released through fast diffusion while the diffusion rate decreases as this ratio gets closer to 1. On the other hand, a change is mesh size is required in order to release the drug content whenever the size of drug molecule is larger than the mesh size. Thus, a control over the mesh size needs to be achieved via internal or external stimuli in order to release the drug. Degradation, swelling and deformation of 3D network can be given as examples to stimuli-responsive mesh size tuning mechanisms [23].

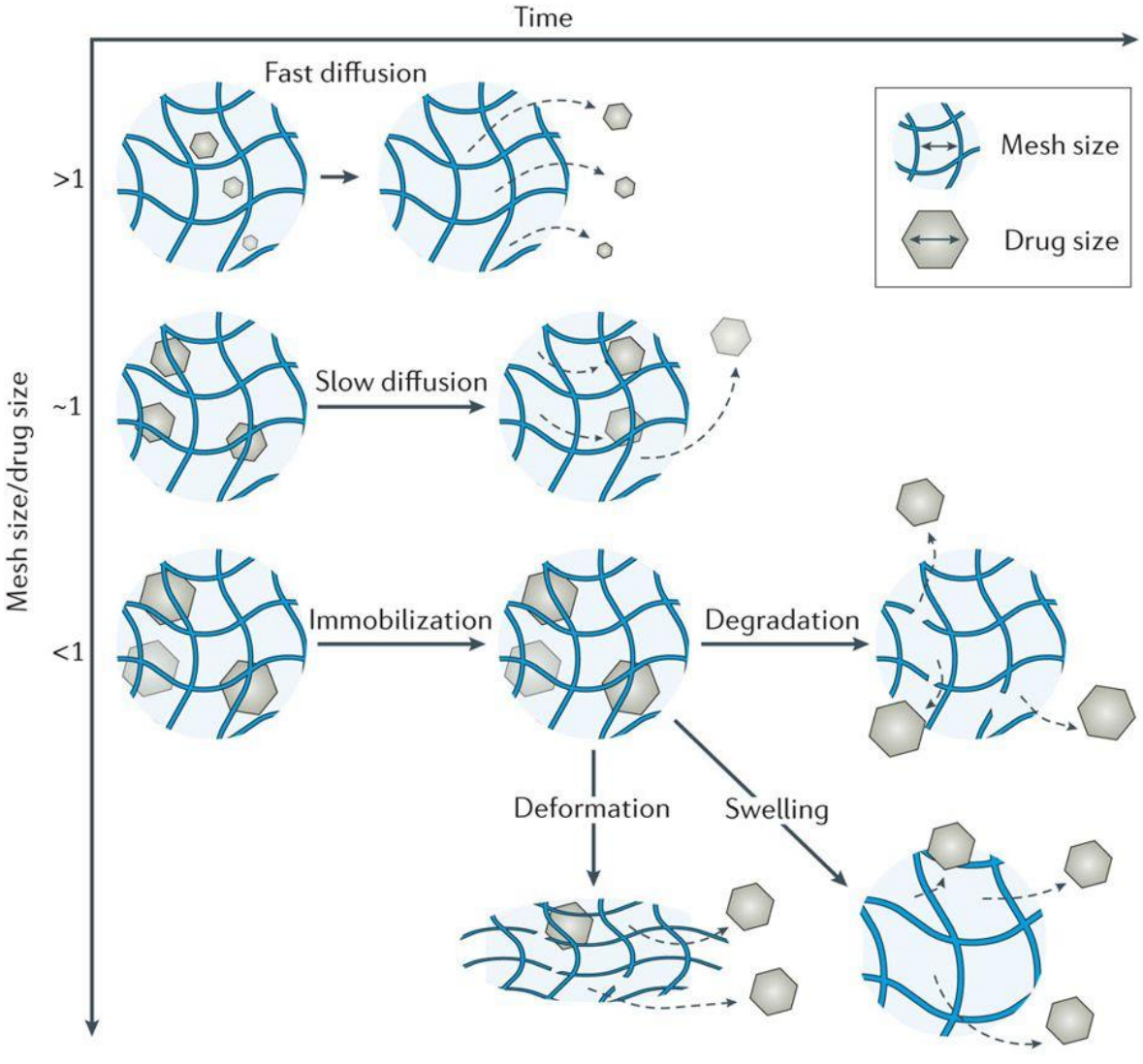

Figure 1.4. Release mechanisms from hydrogels [23].

Another factor determining the rate and extent of drug release is the strategy used for loading the drug into the hydrogel. These strategies can be summarized as covalent conjugation, electrostatic interaction and hydrophobic association (Figure 1.5). Although the last two strategies involve reversible drug loading, cleavable bonds are required to make the first one reversible. This means that the stability of covalent bond between the drug and 3D network will have an impact on the release behavior. Thus, covalent bonds responding to internal stimuli i.e. ester linkages, are useful for tuning the drug release profile of hydrogels [23].

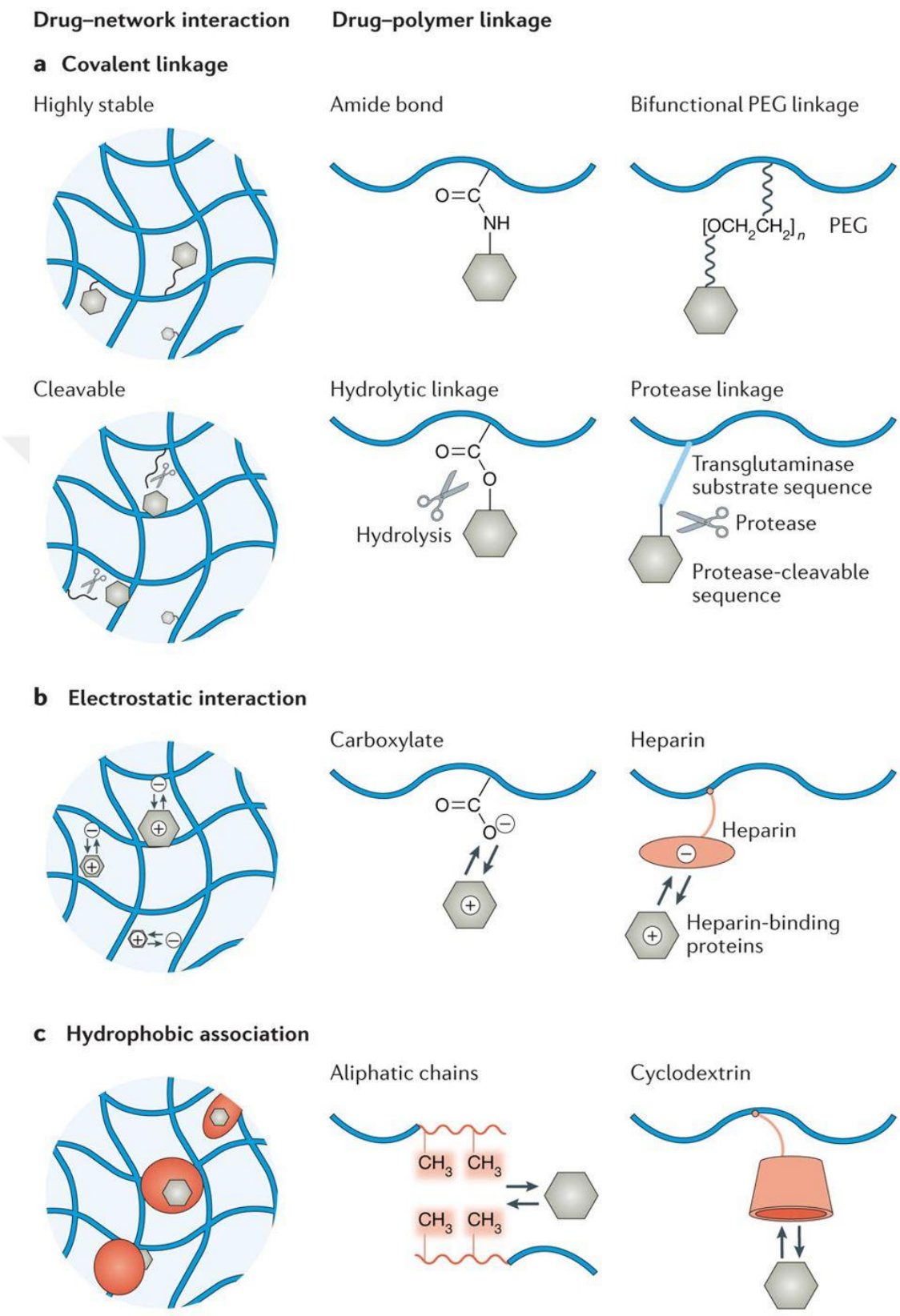

Figure 1.5. Drug-hydrogel interactions [23].

pH sensitive systems are among the most widely studied hydrogel-based drug delivery scaffolds [29]. pH dependent release of drug molecules from these networks can be achieved via different strategies. For instance, hydrogels fabricated from polyelectrolytes such as poly(acrylic acid) (PAA) and poly(N,N′-diethylaminoethyl methacrylate) (PDEAEM) can be utilized for triggered drug release owing to their pH dependent swelling-deswelling behavior [30].

Another common pH-dependent strategy involves use of acidic environment sensitive chemical bonds such as esters, ketals, carbonates and carbamates for the conjugation of the cargo. In a recent study, Sanyal and coworkers designed PEG-based hydrogels and cryogels for sustained and slow release of an anti-cancer drug, namely, Doxorubicin (DOX) [27]. In this study, they synthesized hydrogels and cryogels by UV-mediated polymerization of PEGMEMA, poly(ethylene glycol) dimethacrylate (PEGDMA) and a functionalizable carbonate-NHS monomer (SCEMA). They covalently attached an amine-bearing drug, DOX, through activated-NHS groups post-gelation (Figure 1.6). Then, they compared their drug release profiles at neutral (pH=7.4) and acidic (pH=5.4) environment. They observed that both the porosity of gels and the pH of the surrounding media had an impact on the release profiles of these non-degradable networks. Cryogels having higher porosity than hydrogels showed improved release profiles at both pH values. Importantly, drug release was sustainable and significantly improved at acidic pH due to acid-sensitive hydrolyzable carbamate linker between the drug and the gel. Furthermore, drug-conjugated cryogels were demonstrated to be toxic to MDA-MB-231 cells and the drug content was reported to be tunable.

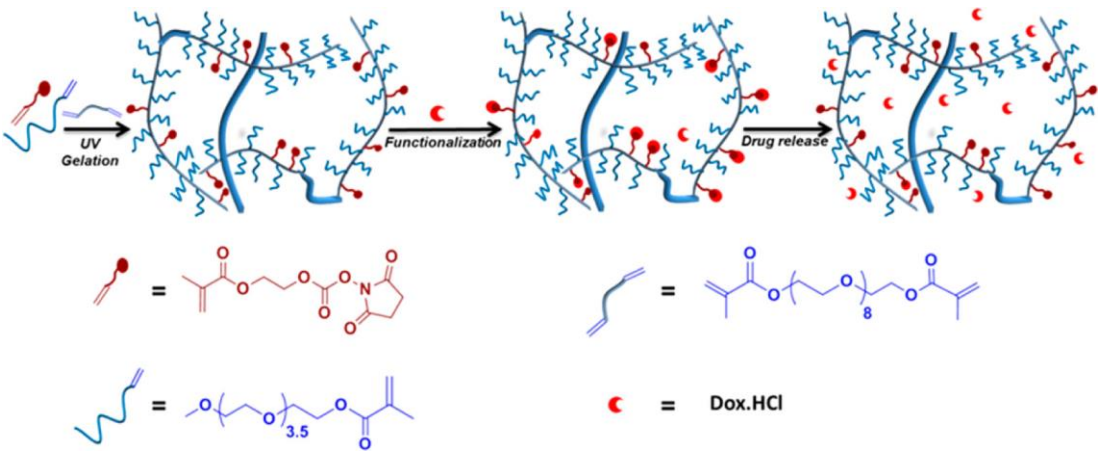

Figure 1.6. pH sensitive DOX releasing hydrogels [27].

pH sensitive drug delivery strategies are not limited to swelling/deswelling equilibrium or acid sensitive linkers for drug conjugation; controlled release via degradation of hydrogels can also be considered. For instance, Wang and Dong and coworkers designed DOX-loaded injectable hydrogels with pH-dependent phase transition behavior for the treatment of human fibrosarcoma [26]. For the synthesis of hydrogels they utilized two biocompatible polymers; dibenzaldehyde-functionalized PEG and polyaspartylhydrazide and crosslinked them through dynamic acylhydrazone bond formation. Since acylhydrazone is acid labile, resulting hydrogels were shown to be degradable under acidic conditions which is characteristic of tumor tissue. These, hydrogels were both physically and chemically loaded with the anti-cancer drug DOX and the release was shown to be tunable upon change in the pH. Drug loaded hydrogels were reported to have better antitumor efficacy than free DOX against HT1080 xenografts *in vivo* owing to their sustained release profiles.

On the other hand, multi-responsive hydrogels where release of drug molecules depend on more than one stimulus may also be designed [31]. For example, Ghavaminejad and Samarikhalaj and coworkers combined pH and temperature sensitive local drug delivery strategies for chemo-photothermal cancer therapy (Figure 1.7) [32]. In this study, they obtained hydrogels from temperature sensitive pNIPAAm-co-pAAm and they loaded them with polydopamine nanoparticles (DP) to flourish them with photothermal properties. Hydrogels were loaded with the first drug, bortezomib (BTZ), through conjugation of catechol and boronic acid moieties in DP and BTZ, respectively. This conjugation was reported to be acid sensitive and release the BTZ in acidic environment which is expected from the tumor tissue. Also, a second drug, DOX, was loaded through physical interactions. DOX release was reported to be on-demand upon deswelling of hydrogels with increase in temperature. Thus, this design combined photothermal therapy achieved by DP with multi-drug chemotherapy obtained in a pH and temperature-controlled manner. This construct was also shown to be efficacious on CT26 colon cancer cell *in vitro*.

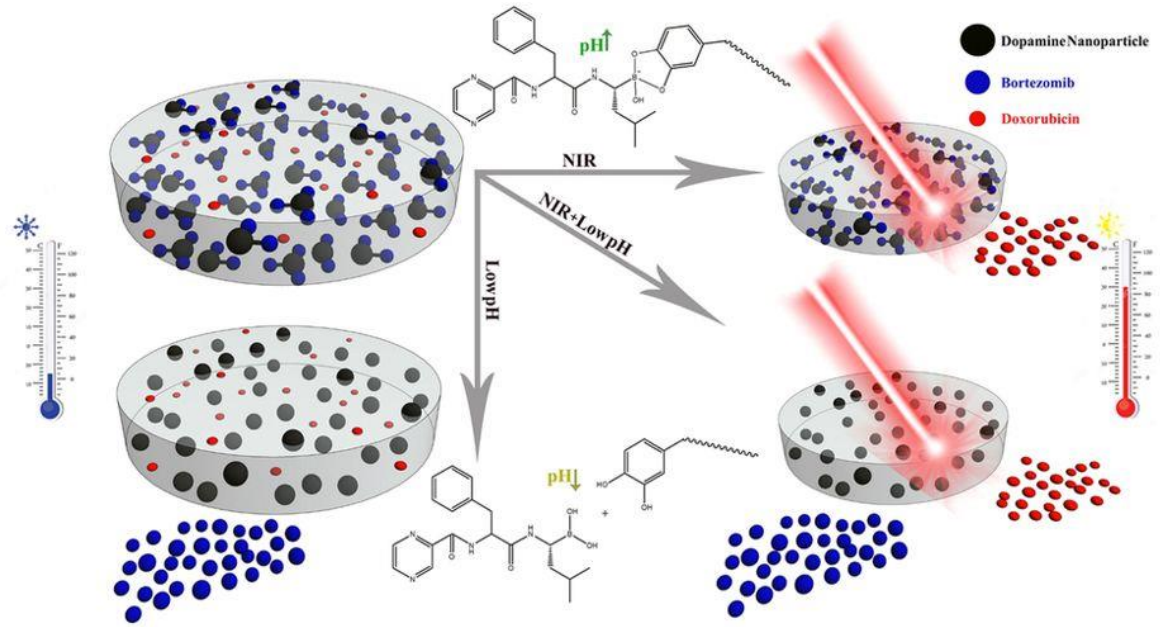

Figure 1.7. pH and NIR mediated release of drugs [32].

Besides the controlled release kinetics, degradation of the drug loaded vehicle after delivery of the cargo is desired whenever it minimizes the amount of surgical interventions in biological applications. Researchers rose to this challenge by introducing temperature [33], matrix metalloproteinase (MMP) [34], ultrasound [35] and redox [36] cleavable polymers and crosslinkers into hydrogel networks. For instance, in a recent work, He *et al*. obtained injectable and degradable hydrogels from thiol-modified hyaluronic acid (HA) (Figure 1.8) [36]. These self-crosslinking hydrogels were loaded *in situ* with three anti-cancer drugs (DOX, Sorafenib and Metformin) for combinatorial therapy and their synergistic behavior was investigated. The release trend was shown to depend on dithiothreitol (DTT) concentration, leading to degradation of 3D network by reduction of disulfide bonds followed by faster release at higher DTT concentrations. Furthermore, this degradable multi-drug delivery construct was reported to show synergistic and apoptotic effect *in vitro* as well as enhanced antitumor efficacy *in vivo* against breast cancer.

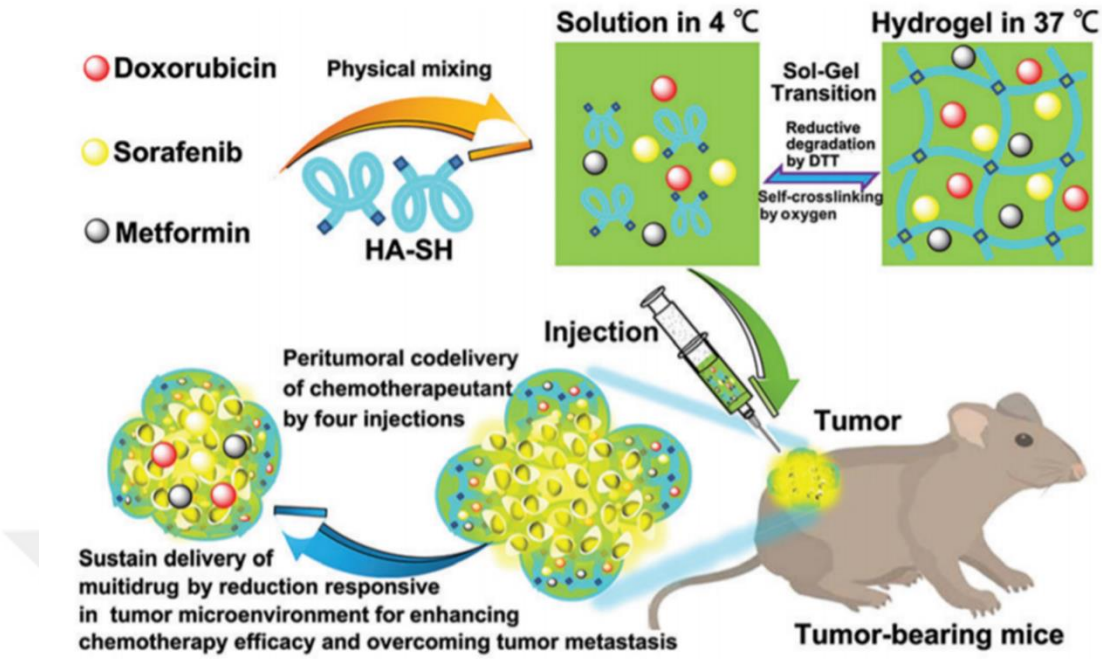

Figure 1.8. Degradable hydrogels for multi-drug delivery.[36]

2. AIM OF THE STUDY

In this study, we aimed to synthesize degradable hydrogels which can be chemically functionalized with drug molecules for local delivery in cancer therapy. For this purpose, we first synthesized a PEG-based copolymer bearing side chains with activated NHS carbonate groups via RAFT polymerization. PEG-based polymers were chosen due to their excellent biocompatibility, hydrophilicity, low toxicity and anti-biofouling properties in biological applications. In order to control the physical properties and microstructure of hydrogels, the crosslinker was chosen as a variable. 3 types of hydrogels were obtained by crosslinking this copolymer by PEG-based crosslinkers with different lengths and their physical properties were compared. The main purpose of varying the length of crosslinker was to tune degradation rates of hydrogels by simply changing their porosity. The reason behind this control over porosity stemmed from our desire for controlling DOX release behavior of hydrogels which was expected to largely depend on degradation trend. Thus, after obtaining hydrogels with unsimilar properties, an anti-cancer drug, DOX, was conjugated onto hydrogels through covalent bonds. The aim here was to obtain a sustained release profile extending for days which is difficult to get via physically drug loaded systems. Since tumor tissue is known to be slightly acidic and rich in glutathione (GSH) compared to healthy tissue, reducible disulfide bonds and acid labile carbamate linkers were utilized for both crosslinking and drug conjugation. Thus, dual-stimuli responsive degradable hydrogels were obtained for local drug delivery.

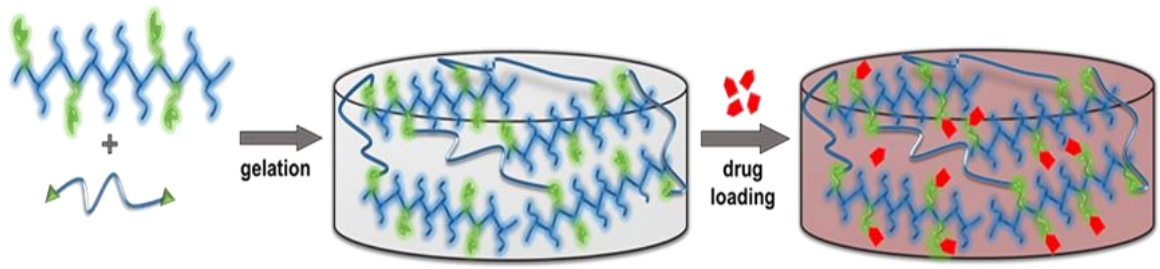

Figure 2.1. Schematic representation of hydrogel synthesis and functionalization.

3. EXPERIMENTAL

3.1. Materials

N,N′-Disuccinimidyl carbonate (DSC, >95%), PEGMEMA, 99%, M_n= 300 g/mol), 2,2′-azobis(2-methylpropionitrile) (AIBN), 2-Cyano-2-propyl dodecyl trithiocarbonate (CTA, 97%), poly(ethylene glycol) diamine (NH_2-PEG2k-NH_2, M_n = 2000 g/mol) and NH_2-PEG6k-NH_2 (M_n = 6000 g/mol) were purchased from Sigma Aldrich. Bis(2-hydroxyethyl) disulfide (90%), triethylamine (99%) and 1-Amino-2-propanol were purchased from Alfa Aesar. Methanesulfonyl chloride (MsCl) (99.7%) and sodium azide were purchased from Sigma Aldrich and poly(ethylene glycol) (PEG, M_n = 10000 g/mol) from Fluka for the synthesis of NH_2-PEG10k-NH_2 (M_n = 10000 g/mol) according to literature.[37] For hydrogel degradation and drug release experiments L-Glutathione reduced (GSH) and Fluoresceinamine, isomer I were purchased from Sigma Aldrich and 1,4-Dithio-DL-threitol (DTT) (98%) was obtained from Alfa Aesar. Chemicals were used as received throughout experiments unless otherwise stated. Solvents were purchased from Merck.

3.2. Instrumentation

SCEDEMA, copolymer and PEG diamine (M_n = 10,000 g/mol) were characterized using ^{1}H-NMR (Avance III HD, 400 MHz, Bruker). The molecular weight distribution of the copolymer, poly(PEGMEMA-*co*-SCEDEMA), was determined by gel permeation chromatography (GPC, Shimadzu) using a PSS-SDV column (Gramlinear, length/ID 8 × 300 mm, 10 μm particle size) calibrated with poly(methyl methacrylate) (PMMA) standards using a refractive-index detector. Dimethylacetamide (DMAc) was used as eluent at a flow rate of 1 mL/min at 30 °C. Functionalizable hydrogels and DOX conjugated hydrogels were characterized by attenuated total reflection Fourier transform infrared (ATR-FT-IR) spectroscopy (Nicolet 380, Thermo Scientific). Scanning electron microscopy (SEM, JCM-5000 NeoScope, JEOL) was used for investigating the morphologies of hydrogels at an accelerating voltage of 10 kV. Physical properties and degradation trends of hydrogels were

investigated using a rheometer (MCR 302, Anton PAAR). Quantitative analysis of Doxorubicin conjugation and release were done by LC-MS/MS (LCMS-8030, Shimadzu) equipped with a C18 column (length/ID 100 x 3 mm, 2.7 μm). Ultra-pure water containing 0.05% ammonium acetate and 0.02% formic acid, and HPLC grade ACN were the mobile phase components. The method was as following; 0 min, 10% ACN; 0.5-4 min, 10% ACN; 4 min, 95% ACN; 5 min, 95% ACN; 5.01-8 min, 10% ACN with a flow rate of 0.5 mL/min. At positive mode, m/z values for doxorubicin precursor and products were 543.50, 397.50, 361.50 and 355.50, respectively.

3.3. Synthesis of SCEDEMA

A two step synthesis route was followed to synthesize SCEDEMA. First, HSEMA was synthesized from bis(2-hydroxyethyl) disulfide at one end and then functionalized with carbonate-NHS using DSC according to previous methods in literature [43]. The monomer was characterized by ^{1}H-NMR.

3.4. Copolymerization of SCEDEMA with PEGMEMA

Reversible addition fragmentation polymerization (RAFT) technique was used for synthesizing the random copolymer. Briefly, PEGMEMA (400 mg, 1.33 mmoles), SCEDEMA (155.6 mg, 0.43 mmoles), CTA (16.48 mg, 0.048 mmoles) and AIBN (0.78 mg, 0.0048 mmoles) were dissolved in anhydrous dioxane (1.8 mL) in a sealed round bottom flask. The reaction flask was purged with N_2 for 20 min to remove the residual oxygen. The polymerization was carried out at 70 °C for 24 h. The reaction was stopped by air exposure and fast cooling after 24 h. The resulting polymer, poly(PEGMEMA-*co*-SCEDEMA), was concentrated via rotary evaporation and precipitated in cold diethyl ether for purification. The precipitate was dried in *vacuo* and characterized using GPC and ^{1}H NMR. ^{1}H NMR (400 MHz, $CDCl_3$, δ, ppm), 4.59 (s, 2H, OCOOCC*H*$_2$CH$_2$S), 4.22 (s, 2H, COOCC*H*$_2$CH$_2$S), 4.08 (s, 2H, COOC*H*$_2$CH$_2$O), 3.38 (s, 3H, OC*H*$_3$), 3.05 (s, 2H, OCOOCCH$_2$C*H*$_2$S), 2.96 (s, 2H, COOCH$_2$C*H*$_2$S), 2.86 (s, 4H, NHS H's).

3.5. Synthesis of Hydrogels

3.5.1. Optimization of Crosslinker Ratio

Hydrogels with varying crosslinking density were snythesized by combining poly(PEGMEMA-*co*-SCEDEMA) and PEG-diamine (PEG6k, M_n = 6000 g/mol) at 8:3, 8:4 and 8:5 NHS:NH_2 ratios. For example, to prepare hydrogels with 8:4 NHS:NH_2 ratio (G2), 10 mg of PEG6k was mixed with 10 mg of copolymer in 1,4-dioxane at a final concentration of 50% wt/V. This mixture was vortexed for 3 sec at high speed and left for 12 h at room temperature for complete gelation. Hydrogel formation was concluded from vial inversion test. Unreacted hydrogel precursors and by-products were removed by washing the hydrogels several times with excess 1,4-dioxane. Then, they were dried *in vacuo*. Hydrogels with 8:3 (G1) and 8:5 (G3) NHS:NH_2 ratio were obtained similarly.

3.5.2. Synthesis of Functionalizable Hydrogels

The NHS:NH_2 ratio was fixed to 8:5 for the fabrication of functionalizable hydrogels. Three different types of hydrogels (HG2k, HG6k and HG10k) were synthesized by varying the length of crosslinker, namely, PEG-diamine. For instance, HG2k hydrogels were fabricated from poly(PEGMEMA-*co*-SCEDEMA) and PEG-diamine (PEG2k, M_n = 2000 g/mol) at a fixed NHS:NH_2 ratio of 8:5. Briefly, 15 mg of copolymer was mixed with 6.25 mg of PEG2k at a final concentration of 50% wt/v in 1,4-dioxane. The mixture was vortexed for 3 sec at high speed and left for 12 h at room temperature for complete gelation. Vial inversion test was performed to conclude in hydrogel formation. After 12 h, HG2ks were washed with excess 1,4-dioxane to remove unreacted polymers and by products. They were dried *in vacuo* before further use.

HG6k and HG10k were prepared similarly at a fixed NHS:NH_2 ratio of 8:5 using PEG-diamine with a number average molecular weight of 6000 g/mol (PEG6k) and 10000 g/mol (PEG10k), respectively, as crosslinker.

3.5.3. De-functionalization of Hydrogels

The carbonate-NHS functional groups on hydrogels were eliminated for characterization studies such as swelling, microstructure analysis, rheological behavior and degradation trend in order to prevent any fluctuation in measurements due to highly reactive functional groups. For this purpose, functionalizable HG2k, HG6k and HG10k hydrogels were treated with 1-amino-2-propanol to eliminate carbonate-NHS. For instance, HG2k was swollen in 3 mL of DCM and 2 equivalents of 1-amino-2-propanol with respect to 1 equivalents of carbonate-NHS in the starting copolymer which should remain after hydrogel formation was added. The reaction took place at room temperature. After 12 h, hydrogels were washed with excess DCM to get rid of excess reactants and by-products. They were then washed with 1,4-dioxane and water, respectively and lyophilized for further use. De-functionalization of HG6ks and HG10ks was performed similarly.

3.6. Characterization of Hydrogels

3.6.1. Gelation Yields

Hydrogels dried *in vacuo* were used for conversion calculations. The gelation yield was equal to $(W_{dry}/W_{p+c})*100$ where W_{dry} was the weight of dried hydrogel and W_{p+c} was equal to the sum of weight of copolymer and crosslinker used for hydrogel fabrication.

3.6.2. Swelling Studies

The water uptake of HG2k, HG6k and HG10k were measured gravimetrically. For instance, 10 mg samples of HG2k which were previously lyophilized were swollen in 5 mL dH_2O at room temperature. They were taken out at pre-determined time points and weighed after removing the excess water on their surfaces via a moisturized filter paper. The swelling measurements were done as triplicates for each type of hydrogel.

3.6.3. Imaging of Microstructure

De-functionalized dry hydrogels were cracked using liquid nitrogen. Microstructure of each type of hydrogel was investigated using SEM at an accelerating voltage of 10 kV. Porosity was investigated and compared for HG2k, HG6k and HG10k.

3.6.4. Determination of Functional Groups

The presence of functional groups on hydrogels was investigated by IR spectroscopy. IR measurements were taken before and after treatment with 1-amino-2-propanol.

3.6.5. Rheological Studies

For rheological analysis, 20 mg of hydrogel samples in disk shape were swollen in dH_2O. Frequency sweep test was performed to determine the viscoelastic properties of hydrogels. Hydrogels were subjected to angular frequencies from 0.1 to 100 rad/s at a fixed strain value of 1% at 25 °C while recording storage modulus (G') and loss modulus (G''). Amplitude sweep test was performed to determine the linear viscoelastic (LVE) region of hydrogels where G' and G'' values remain constant. G' and G'' were recorded against strain values from 0.01 to 100% at an angular frequency of 10 rad/s at 25 °C.

3.7. Degradation of Hydrogels

3.7.1. Visual Investigation of Degradation

In order to follow the degradation of hydrogels visually, fluorescein amine conjugated hydrogels were prepared. Briefly, 1.5 equivalents of fluorescein amine (with respect to 1 eq. of NHS in polymer which should remain unreacted after gelation) and 9 equivalents of Et_3N were added onto hydrogels swollen in 3 mL of DCM. The reaction was run for 12 h at room

temperature. After 12 h, fluorescently labeled HG2k (HG2k-FL), HG6k (HG6k-FL) and HG10k (HG10k-FL) were washed several times with excess DCM to remove unreacted dye and by-products. These gels were then dried under *vacuo*.

Next, HG2k-FL, HG6k-FL and HG10k-FL were swollen in 4 mL PBS (pH = 7.4) in the presence of 5 mM glutathione (GSH). They were kept in an incubator shaker at 37°C, 200 rpm. As a control set, HG2k-FL, HG6k-FL and HG10k-FL were kept in PBS using the same conditions. All 6 hydrogels were visualized under UV-light (λ = 365 nm) at 0 h and after 12 h.

3.7.2. Rheological Investigation of Degradation

De-functionalized HG2k, HG6k and HG10k samples of 20 mg were used for following the degradation rheologically. Time sweep test was performed to previously swollen (in dH_2O) hydrogels. First, G' and G'' were recorded at 37 °C in the presence of sodium acetate buffer (NaOAc, pH = 5.5). After 73 min, gels were treated with 50 mM of DTT in NaOAc buffer. G' and G'' were recorded continuously with 30 s increments at an angular frequency of 10 rad/s and a strain value within the previously determined LVE range of hydrogels. For each type of hydrogel, data was taken until crossing of G' and G'' was observed. Degradation plot was obtained by plotting the percent loss in storge modulus against time.

3.8. Conjugation of Doxorubicin to Hydrogels

Doxorubicin was conjugated to NHS functionalized HG2k, HG6k and HG10k hydrogels through carbamate formation. Drug equivalents to be added were calculated with respect to estimated NHS content of the particular hydrogel. This was determined separately for HG2k, HG6k and HG10k assuming that 3 eq. of unreacted NHS remains with respect to 1 eq. polymer used for hydrogelation multiplied by conversion. For example, for 10 mg of HG6k, 10 mg of copolymer was utilized and the gelation yield was 63 %. So, 1.5 eq. DOX.HCl (1.28 mg, 0.00236 mmoles) with respect to 1 eq. NHS (0.00158 mmoles) assuming 6.5 mg of copolymer was weighed into a vial and 3 mL of DCM was added onto

it. Et_3N (3 eq., 0.52 µL) was added into the reaction mixture and the mixture was incubated at 250 rpm, 25 °C for 5 min. Then, dry HG6k was added and the reaction was run for 12 h without changing the conditions. After 12 h, the reaction solution was collected and evaporated by rotary evaporation. The gel was washed several times with DCM until no DOX was detected in the washing solution. The gel was then washed with 1,4-dioxane and water, respectively. Drug conjugated hydrogel (HG6k-D) was lyophilized and characterized by IR spectroscopy. Same protocol was used for conjugation and characterization of DOX in HG2ks (HG2k-D) and HG10ks (HG10k-D).

3.9. pH and Redox Dependent Release of Doxorubicin from Hydrogels

To investigate the release trends of HG2k-D, HG6k-D and HG10k-D hydrogels, 3 conditions were utilized: PBS (pH = 7.4), acetate buffer (pH = 5.5) and acetate buffer supplemented with 5 mM GSH. Briefly, HG6k-D was cut into 2.5 mg pieces and each piece was put into a dialysis membrane (regenerated cellulose, molecular weight cut-off = 3.5 kDa) with 500 µL of relevant medium (i.e. PBS). Hydrogel bearing dialysis membrane was put into a vial and covered with 3 mL of relevant medium. The vial was placed to an incubator shaker at 37 °C, 200 rpm to initiate the release. 100 µL of sample was taken and diluted 1:10 in ACN:dH_2O (1:1) at pre-determined time points and analyzed by LC/MS-MS using previously indicated method. The remaining medium was decanted and 3 mL of fresh relevant medium was added at each measurement point after sampling. Release studies were performed at the same time for all 3 conditions as triplicate experiments.

Cumulative release percent was calculated as following. The released DOX was quantified via LC/MS-MS. Measurements were done up to 12 days until there were no further release of DOX out of the dialysis membranes. Then, the medium outside of the membrane was taken out. The membrane was cut and the sample inside the membrane was treated with 1 mL of 100 mM DTT for 2 h in order to quantify DOX which was not released. Total amount of drug was calculated as the sum of the DOX released and DOX in the membrane. Cumulative release (%) was calculated as the total drug released until the specific time point over total DOX loading multiplied by 100. DOX release was investigated similarly for HG2k-D and HG10k-D hydrogels.

4. RESULTS AND DISCUSSION

4.1. Synthesis and Characterization of poly(PEGMEMA-co-SCEDEMA)

Functionalizable copolymer, poly(PEGMEMA-*co*-SCEDEMA), was synthesized by reversible addition fragmentation polymerization (RAFT) of a PEG-based monomer, namely, PEGMEMA and a disulfide bridge bearing carbonate-NHS monomer (SCEDEMA) (Figure 4.1). PEGMEMA was chosen as a comonomer due to its hydrophilicity and anti-biofouling properties. SCEDEMA generated the functionalizable sites on the copolymer which were necessary for hydrogelation and drug conjugation post-hydrogelation. Owing to the low polydispersity index (PDI) and low toxicity of synthesized polymers in biological environment, RAFT was chosen as the polymerization technique [38].

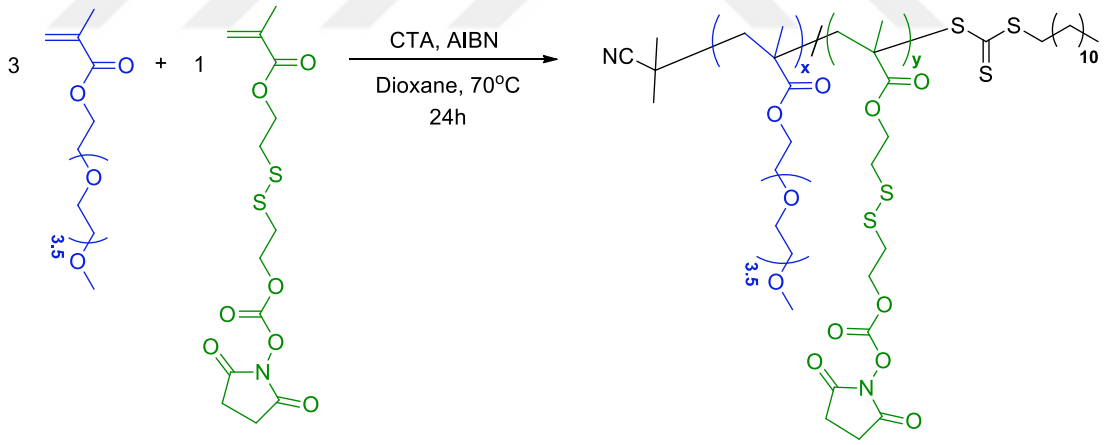

Figure 4.1. Synthesis of poly(PEGMEMA-*co*-SCEDEMA).

A fixed feed ratio of 3:1 of PEGMEMA to SCEDEMA was used for random copolymer synthesis. The resulting poly(PEGMEMA-*co*-SCEDEMA) was calculated to have a PEGMEMA to SCEDEMA ratio of 4:1 from the relation of methoxy protons in PEGMEMA at 3.38 ppm and NHS protons at 2.86 ppm in ^{1}H-NMR spectrum (Figure 4.2). Poly(PEGMEMA-*co*-SCEDEMA) was synthesized with 75 % yield and had a number average molecular weight (M_n) of 12000 g/mol with a PDI of 1.3 as deduced from gel

permeation chromatography (GPC) (Figure 4.3). From the combination of GPC and ^{1}H-NMR analyzes, the resulting copolymer was concluded to have 8 carbonate-NHS functional groups per polymer chain.

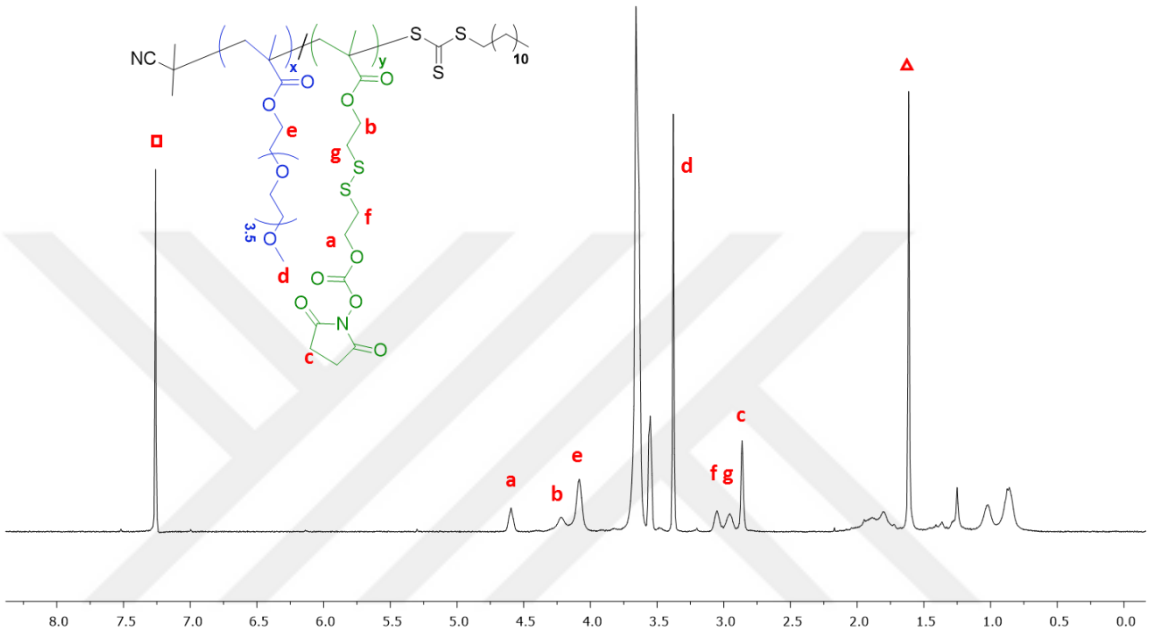

Figure 4.2. ^{1}H-NMR of carbonate-NHS bearing copolymer (Δ: water, □: chloroform).

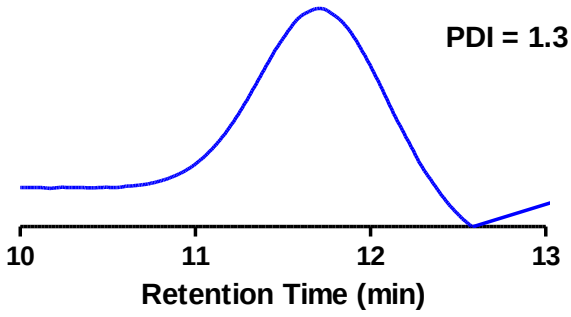

Figure 4.3. GPC trace of poly(PEGMEMA-*co*-SCEDEMA) in DMAc.

4.2. Fabrication of Functionalizable Hydrogels

Functionalizable hydrogels were synthesized by combination of poly(PEGMEMA-*co*-SCEDEMA) with a hydrophilic crosslinker, namely, PEG-diamine (M_n = 2000, 6000 and 10000 g/mol) (Figure 4.4).

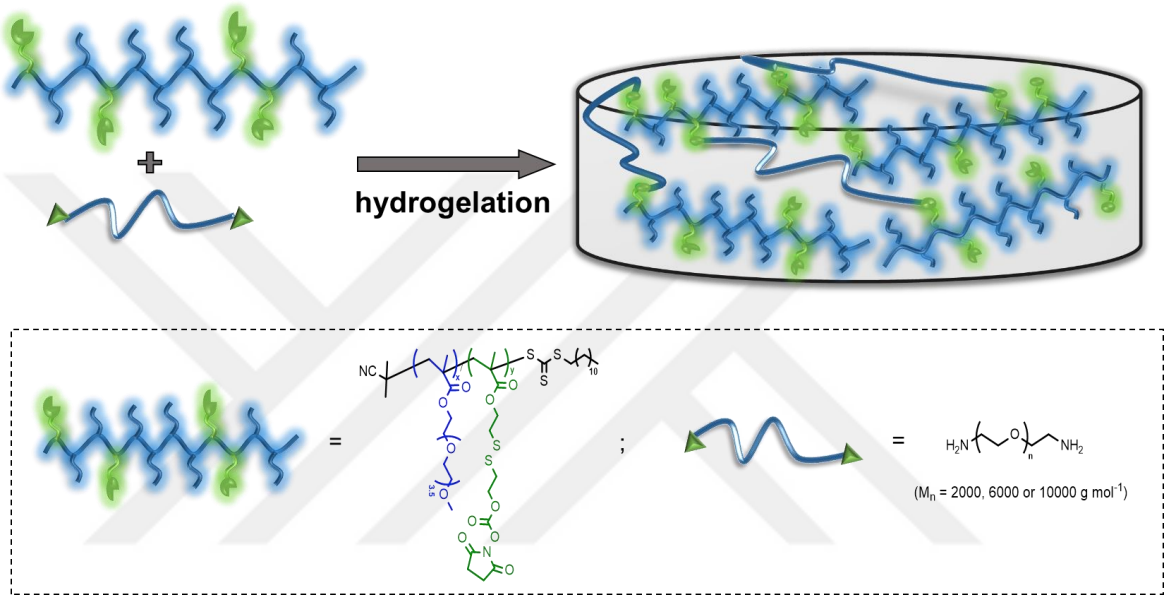

Figure 4.4. Schematic illustration of hydrogel synthesis.

Hydrogelation was achieved through alkoxycarbonylation of primary amines coming from the crosslinker by activated carbonyl groups on the side chains of copolymer. Thus, crosslinking was achieved through carbamate formation. Importantly, this crosslinking mechanism did not involve any toxic by-products which may remain and cause toxicity in biological applications [39]. Furthermore, this strategy provided carbamate and disulfide groups at the crosslinking sites which rendered the hydrogels pH and redox sensitive at the same time (Figure 4.5).

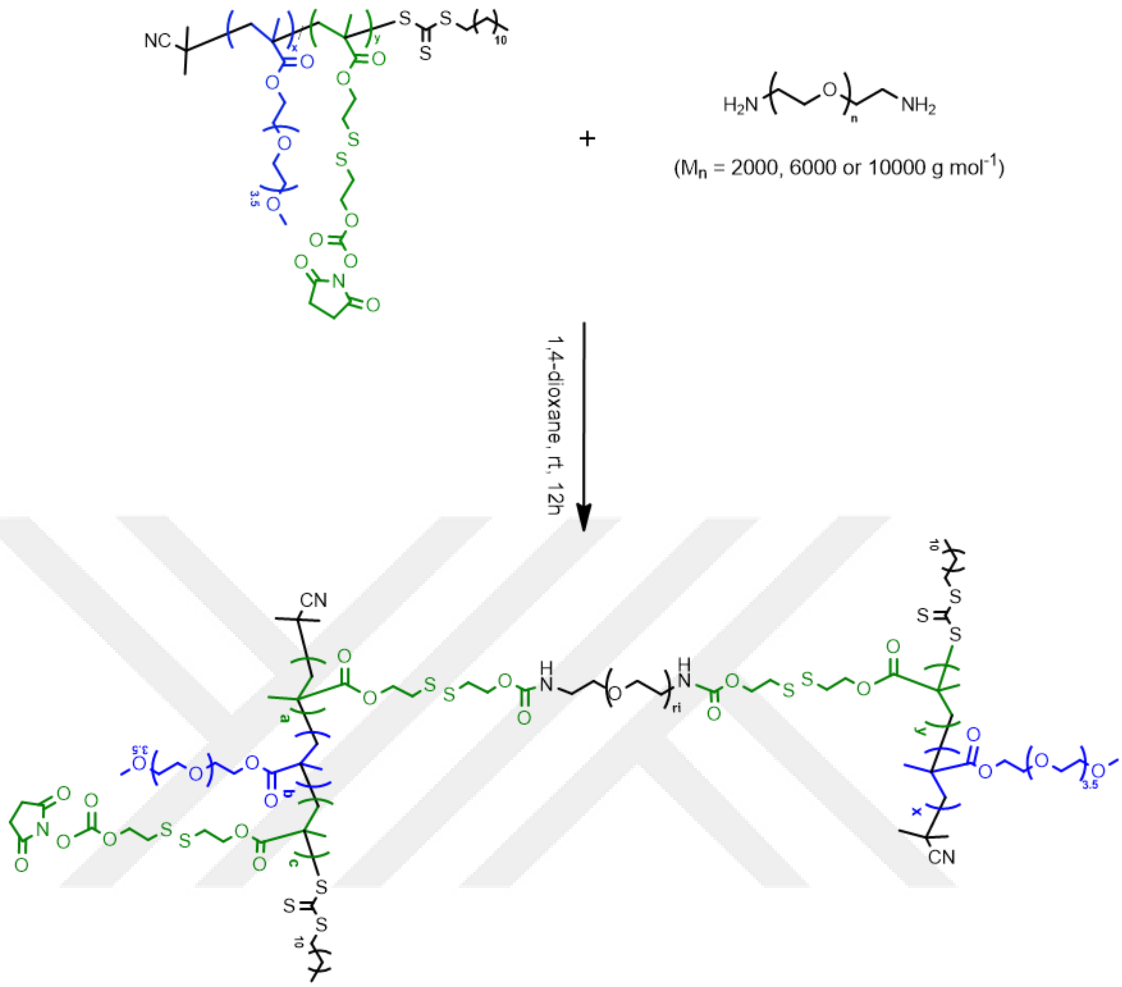

Figure 4.5. Synthesis of hydrogels.

On the other hand, hydrogelation yields are affected by experimental conditions such as temperature, concentration, crosslinker ratio and length of crosslinker. Thus, these parameters should be finely tuned in order to obtain hydrogels with acceptable yields. For this reason, we first optimized the NHS:NH_2 ratio using PEG-diamine (M_n = 6000 g/mol, PEG6k) as crosslinker and kept the total polymer concentration at 50 % (w/v). Crosslinker amount was calculated according to the ratio of NHS groups which were present on poly(PEGMEMA-*co*-SCEDEMA) to NH_2 groups found on crosslinker. As shown in Table XX, conversion was too low with 21 % and 25 % for hydrogels obtained at an NHS:NH_2 ratio of 8:2 and 8:3, respectively. However, increasing the amount of crosslinker enhanced the gelation yield up to 63 % for an NHS:NH_2 ratio of 8:5 following the increase in number of crosslinking sites. Due to highest conversion and theoretically still remaining functional

groups, 8:5 NHS to NH_2 ratio was chosen to proceed with for the rest of the hydrogel synthesis steps in this work.

Table 4.1. Formation of 6k Hydrogels with Different Crosslinker Ratios

Sample	Total Polymer Concentration	NHS:NH_2 Mole Ratio	Crosslinker	Conversion
G1	50% (wt/v)	**8:2**	PEG6k	21 %
G2	50% (wt/v)	**8:3**	PEG6k	25 %
G3	50% (wt/v)	**8:4**	PEG6k	45 %
G4	50% (wt/v)	**8:5**	PEG6k	63 %

Chemical and physical conditions used for hydrogelation not only affect the gelation yield but also physical properties of hydrogels such as porosity, water uptake, viscoelastic behavior and degradation trend. Most importantly, these hydrogels can be tuned to have different drug release profiles by varying only a single parameter such as length of the crosslinker. Thus, varying the length of the crosslinker is expected to result in hydrogels with different porosity, swelling, physical strength and degradation trends, which in turn will lead to a difference in drug release profiles. In order to study this distinction, after fixing NHS to NH_2 ratio to 8:5, three types of hydrogels were fabricated using PEG-diamine at various lengths (PEG2k, PEG6k and PEG10k with M_n= 2000, 6000 and 1000 g/mol, respectively). Although, hydrogels fabricated from PEG2k, PEG6k and PEG10k (HG2k, HG6k and HG10k, respectively) had similar gelation yields, (62 %, 63 %, and 62 %, respectively) they significantly diverged in their physical properties as it will be elaborated on the following sections.

4.3. Characterization of Functionalizable Hydrogels

Physical properties of HG2k, HG6k and HG10k were investigated and compared in this section.

4.3.1. Comparison of Microstructure

The microstructure of hydrogels was investigated using SEM. Since HG2k hydrogels were fabricated using PEG2k which was the shortest crosslinker amongst the others, they were expected to have the lowest porosity compared to HG6K and HG10k. SEM images of HG2k showed irregular pore distribution with small size which was expected from a bulk hydrogel generated with a short crosslinker (Figure 4.6). Pores in HG2ks became visible only at higher magnifications at 400x and 800x in SEM (Figure XX-c,d).

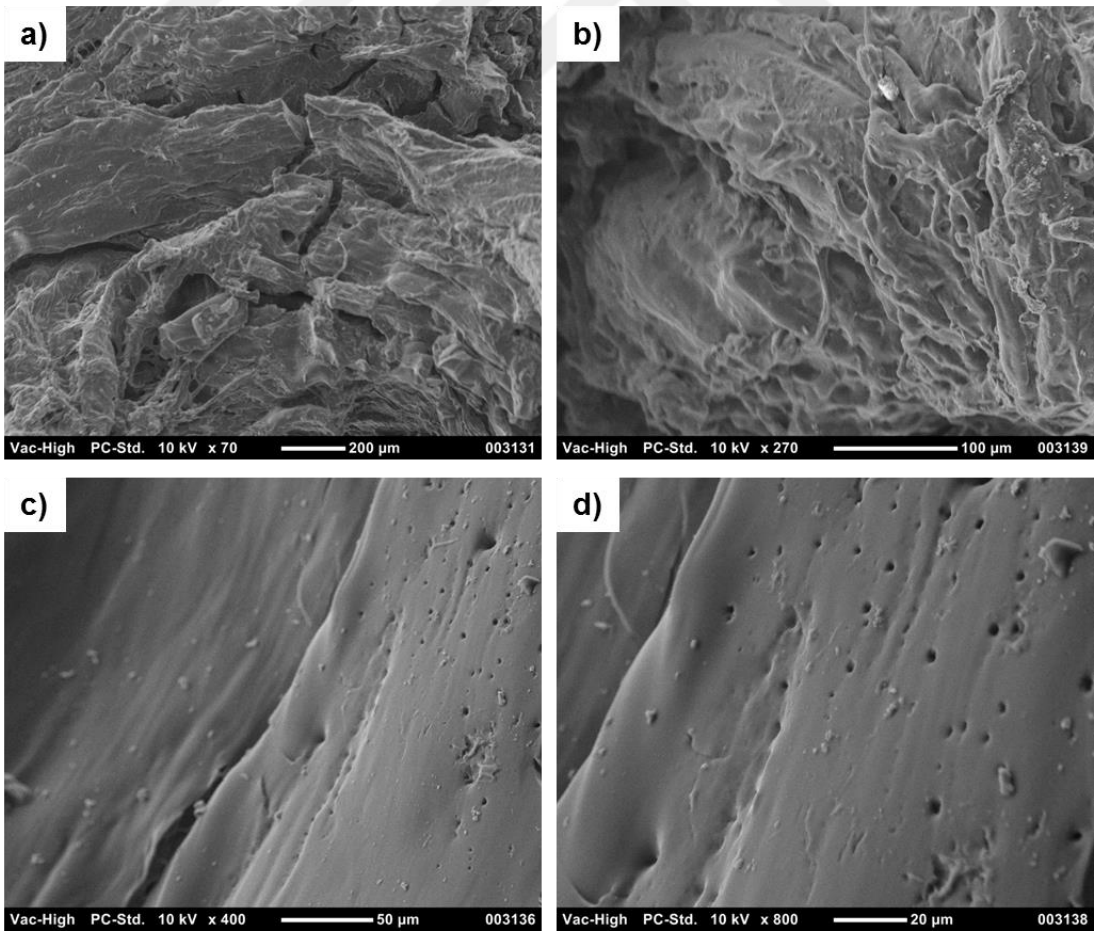

Figure 4.6. SEM images of HG2ks. Scale bar; a) 200 µm, b) 100 µm, c) 50 µm and d) 20 µm.

Consistently, SEM analysis of HG6ks which were synthesized using the middle-sized crosslinker, indicated irregular pore distribution with larger size compared to HG2ks (Figure 4.7). Pores of HG6ks were visible even at 70X magnification (Figure 4.7a) while no porosity was observed in HG2ks at the same resolution (Figure 4.6a).

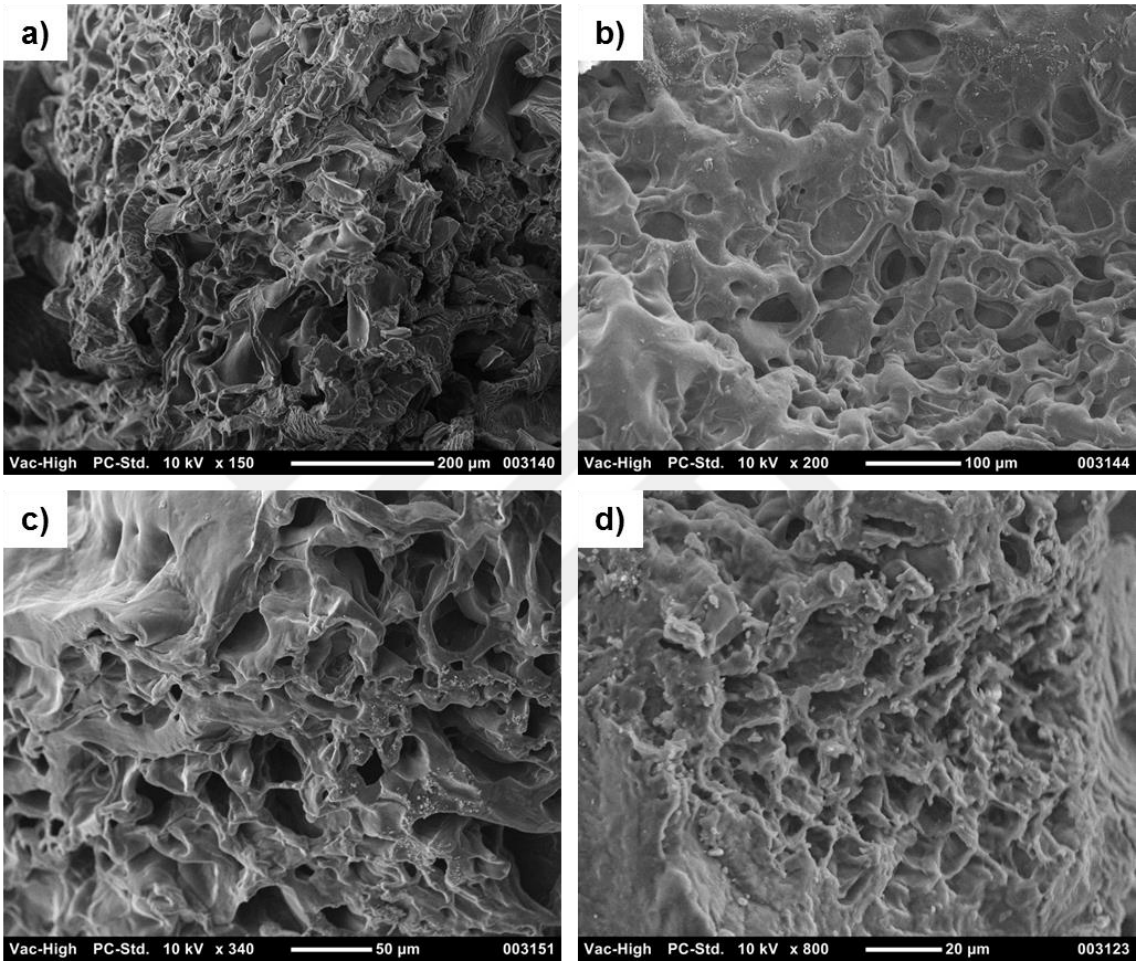

Figure 4.7. SEM images of HG6ks. Scale bar; a) 200 µm, b) 100 µm, c) 50 µm and d) 20 µm.

Lastly, HG10ks fabricated with the longest crosslinker had largest pores as deduced from SEM analysis (Figure 4.8). Pores of HG10k were observable even at lowest magnification of 30X (Figure 4.8a).

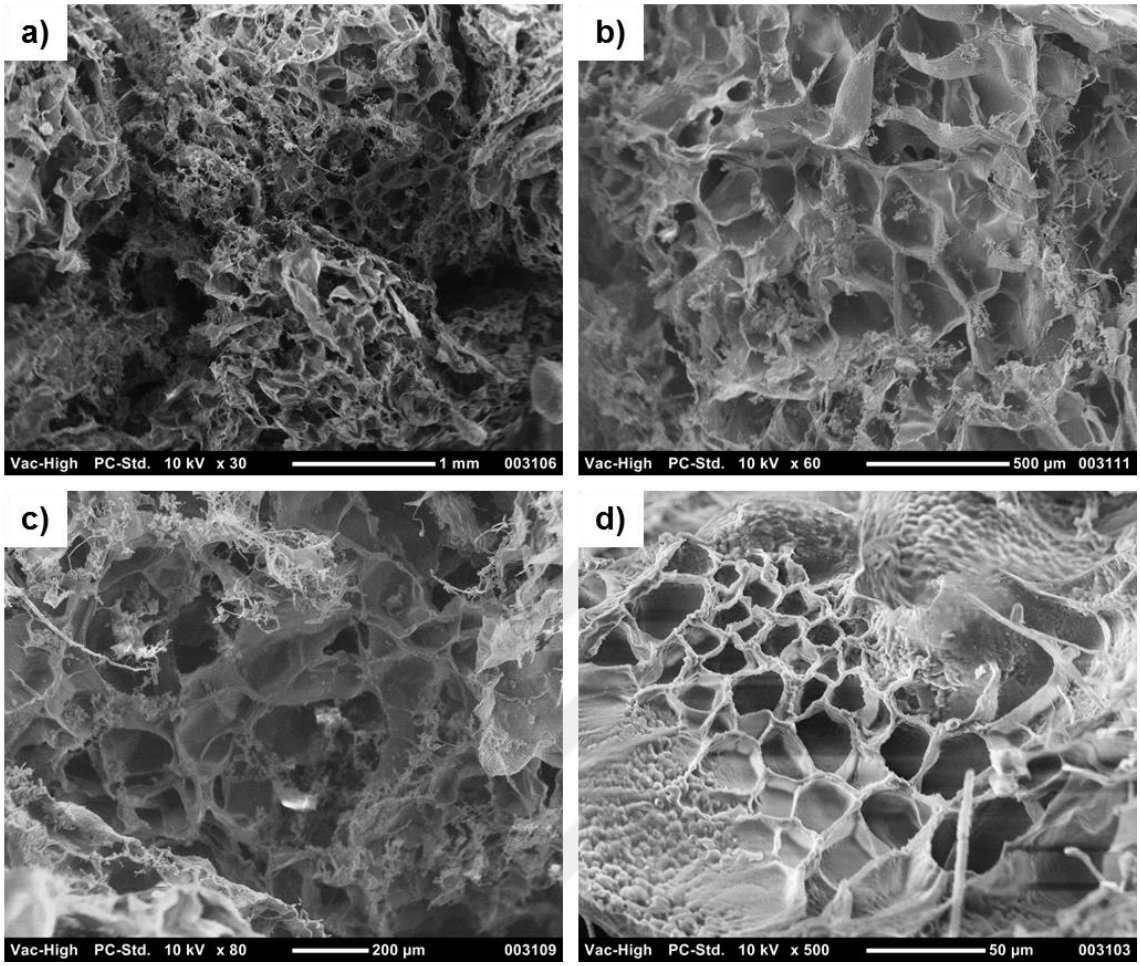

Figure 4.8. SEM images of HG10ks. Scale bar; a) 1 mm, b) 500 µm, c) 200 µm and d) 50 µm.

Thus, the length of the crosslinker was shown to have a considerable effect on the microstructure of resulting hydrogel. The porosity of hydrogels was shown to increase with the increase in the size of crosslinker as indicated by the SEM results.

4.3.2. Swelling Profiles

To follow up on the morphological analysis done by SEM, swelling profiles of HG2k, HG6k and HG10k hydrogels were investigated and compared. From the swelling experiments, HG2k was observed to have the lowest water uptake at equilibrium while HG10k had the highest and HG6k's value was in the middle (Figure 4.9). Thus, water uptake at equilibrium was greatest for hydrogels with highest porosity and vice versa.

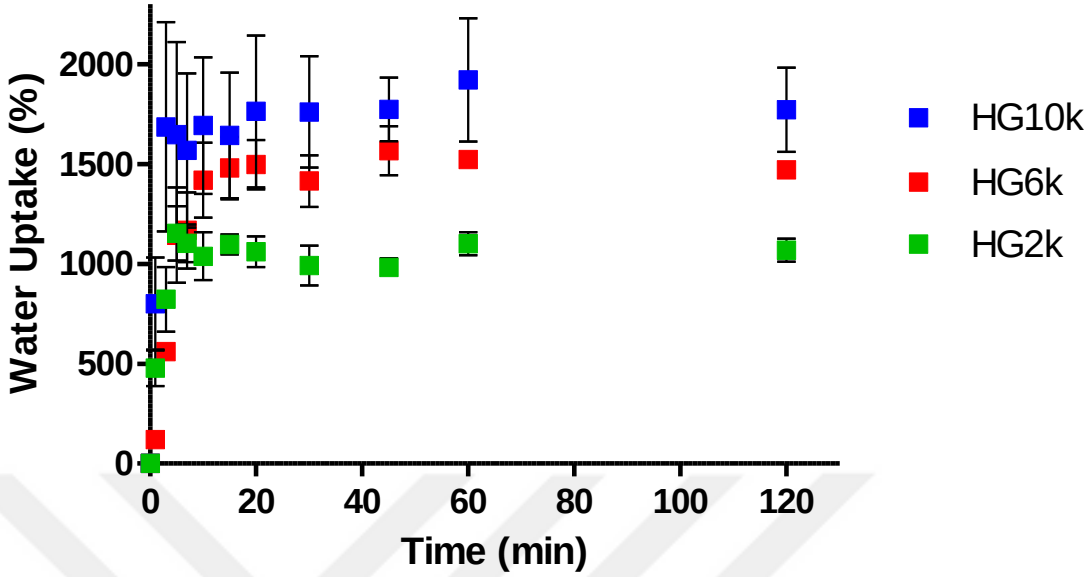

Figure 4.9. Swelling profiles of HG2k, HG6k and HG10k.

4.3.3. Rheological Analyzes

The chain length of crosslinker was also expected to affect the viscoelastic properties of hydrogels besides the microstructure. Rheological analysis was performed to investigate the difference. Since the crosslinking of the polymer network was very fast for all 3 types of hydrogels, hydrogelation could not be followed by time sweep tests. However, mechanical properties of HG2k, HG6k and HG10k were compared via frequency sweep and amplitude sweep tests.

First, the linear viscoelastic (LVE) regions of hydrogels were determined via amplitude sweep tests. The presence and the length of LVE region for hydrogels is an indicator of hydrogel stability [40]. Amplitude sweep test was used for determining the critical strain of hydrogels after which the inversion of G' and G'' occurs meaning the breakage of bonds holding the hydrogel. HG2k (Figure 4.10), HG6k (Figure 4.12) and HG10k (Figure 4.14) hydrogels were observed to resist high oscillatory strains and conserve their gel-like properties. HG2ks having the shortest crosslinker had the strongest mechanical properties with resistance to higher strain values (Figure 4.10).

In addition, higher magnitude of storage modulus compared to loss modulus up to an observed angular frequency value in frequency sweep tests prove that HG2k (Figure 4.11), HG6k (Figure 4.13) and HG10k (Figure 4.15) behave like viscoelastic solid structures rather than liquid. As expected, hydrogels fabricated using the shortest crosslinker (HG2k) had the highest G' value which was higher than 10000 Pa (Figure 4.11) while hydrogels obtained using longest crosslinker (HG10k) had the lowest G' value around 1000 Pa (Figure 4.15). G' for HG6ks was between 10000 Pa and 1000 Pa supporting the conclusion, higher mechanical strength for shortest length of crosslinker. Thus, viscoelastic behavior and stability of hydrogels were shown to be tunable just by changing the size of crosslinker. So, these hydrogels can be adapted to different tissues having separate elastic properties for biomedical applications without changing the polymer and functionality.

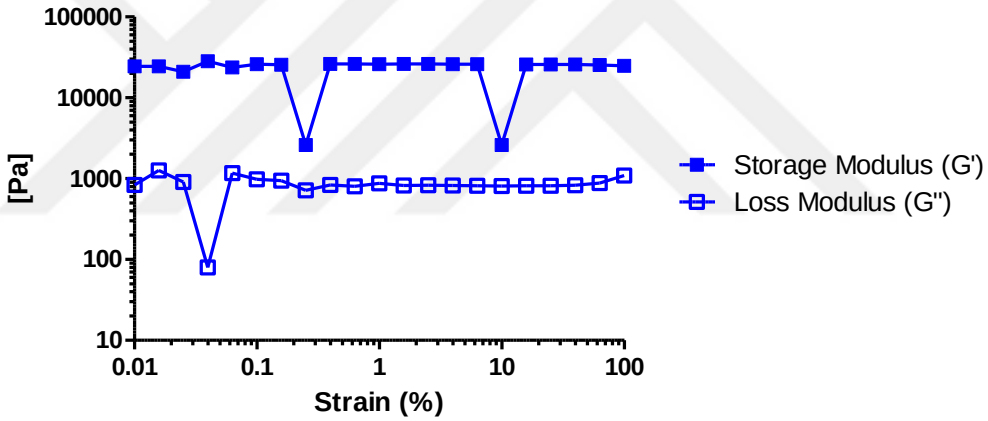

Figure 4.10. Amplitude Sweep Test of HG2k.

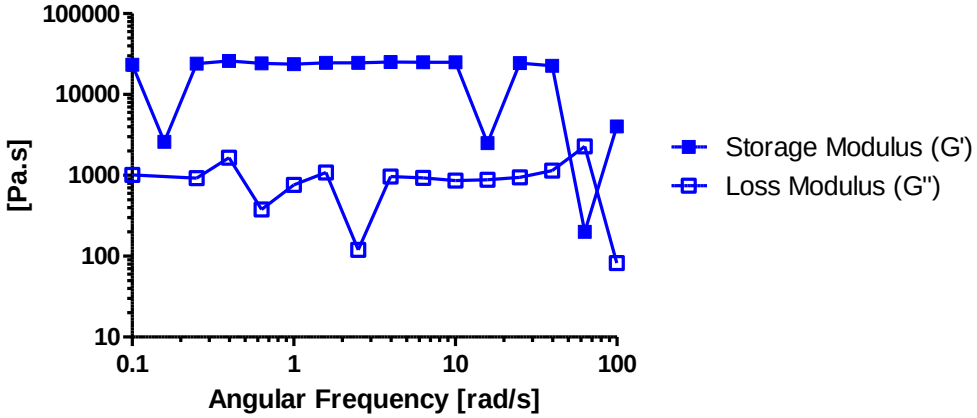

Figure 4.11. Frequency Sweep Test of HG2k.

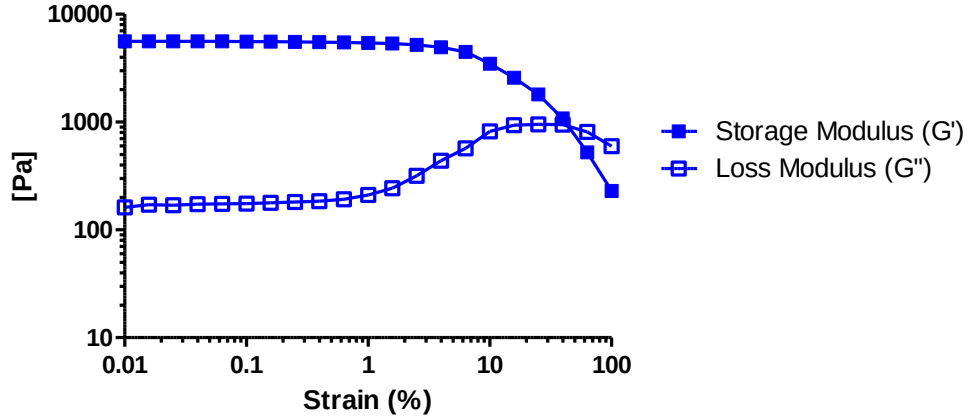

Figure 4.12. Amplitude Sweep Test of HG6k.

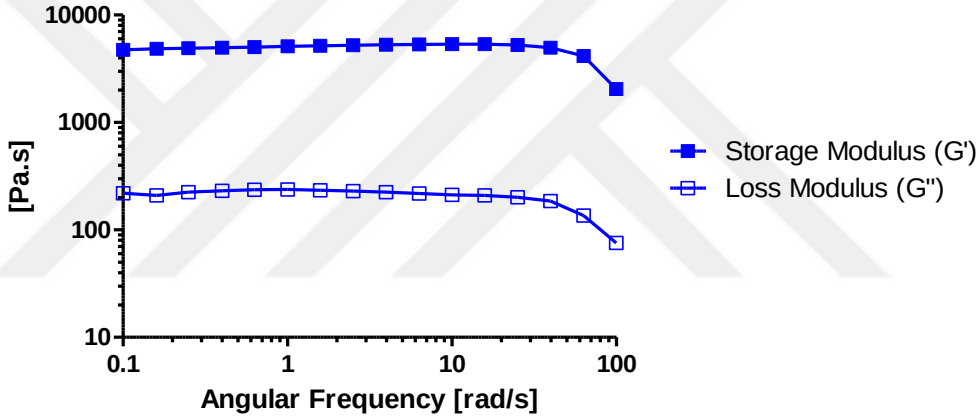

Figure 4.13. Frequency Sweep Test of HG6k.

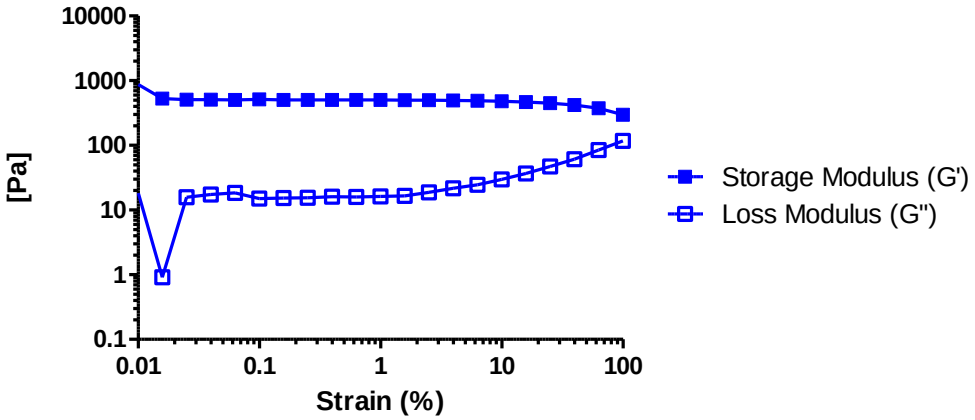

Figure 4.14. Amplitude Sweep Test of HG10k.

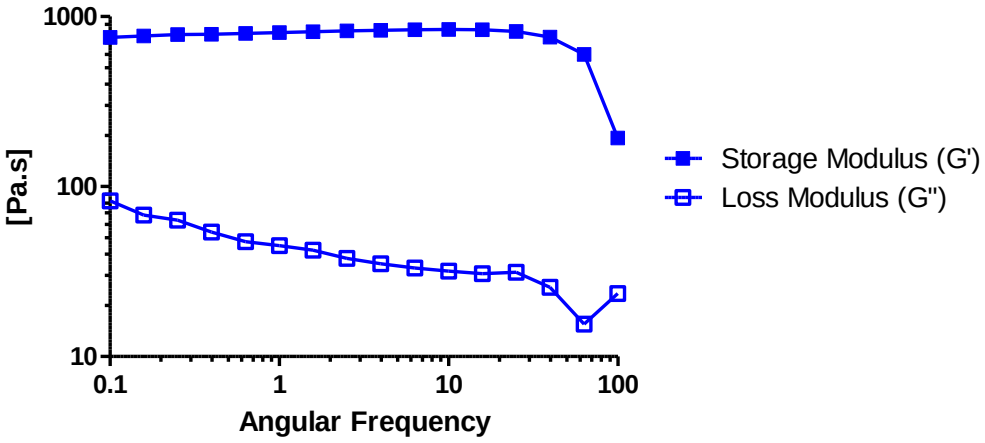

Figure 4.15. Frequency Sweep Test of HG10k.

4.3.4. IR Analyzes

Following the fabrication of hydrogels, the presence of functional groups was determined through IR spectroscopy. C=O stretching peaks at 1812 cm^{-1} and 1789 cm^{-1} in the FT-IR spectra of HG10k (Figure A.1), HG6k (Figure 4.16) and HG2k (Figure A.2) indicated the presence of NHS carbonyls in hydrogels.

Treatment of hydrogels with 1-amino-2-propanol resulted in the disappearance of these peaks further claiming that these hydrogels had NHS functional groups and that these groups were reactive making hydrogels functionalizable.

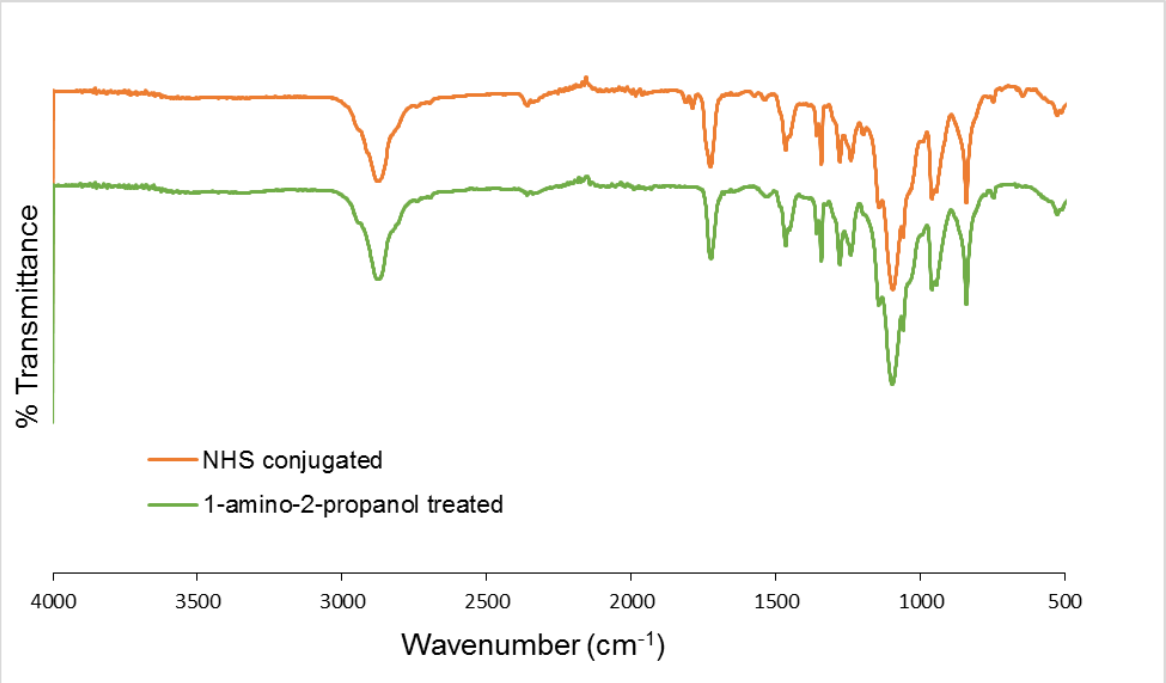

Figure 4.16. FT-IR spectrum of NHS functionalized and 1-amino-2-propanol treated HG6k.

4.4. Degradation of Hydrogels

The aim of the study was to fabricate drug-loaded hydrogel patches that will be introduced after tumor removal upon surgery. For such an application, hydrogels are desired to be degradable so that they could be cleared off from the body after playing their role of local drug delivery without taking an additional surgical action. Thus, as mentioned in the hydrogel fabrication section, hydrogels were designed to be degradable in the presence of a reducing environment. The redox-responsiveness was achieved through introduction of disulfide bridges into the crosslinking sites. Since the products of degradation which were copolymer and the crosslinker are short in length (12 kDa at max.) for all 3 types of hydrogels, they could be cleared off from the body through renal filtration [41].

In addition, the degradation behavior was expected to depend on the size of the crosslinker. In order to investigate the degradation trends of HG2k, HG6k and HG10k hydrogels, both visual and rheological examination was performed. For visualization,

fluorescein amine conjugated HG6k (HG6k-FL) was treated with 5 mM GSH overnight. The photographic images before and after treatment show total fluorescence in case of GSH treated hydrogels due free and/or polymer conjugated drug in solution (Figure 4.17). On the other hand, no fluorescence was observed in the solution without the reducing agent proving that degradation was GSH dependent.

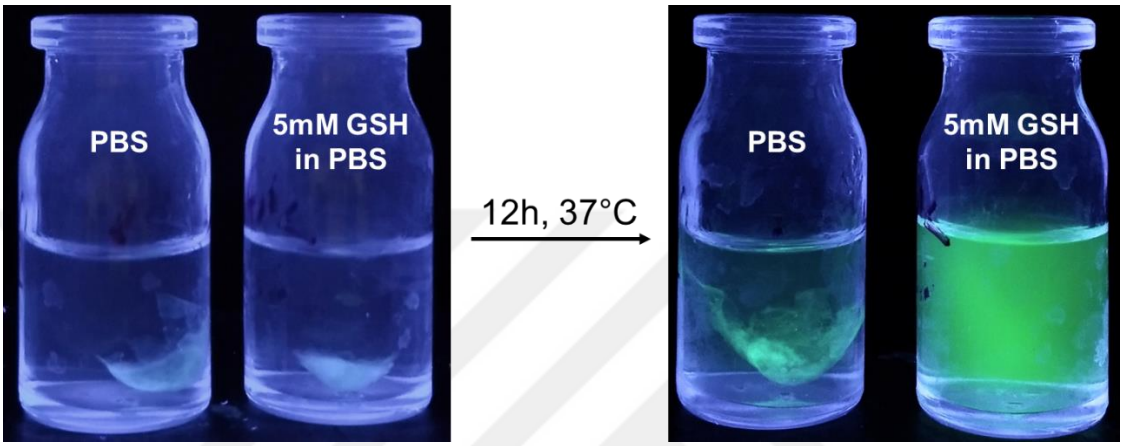

Figure 4.17. Photographic image of degradation of HG6k-FL.

Degradation of HG2k, HG6k and HG10k were followed more delicately via rheological analysis. For this purpose, time sweep test was performed to hydrogels first in the absence and then in the presence of reducing environment. Storage moduli of hydrogels were recorded against time first in acetate buffer (pH = 5.5) then in acetate buffer supplemented with 50 mM DTT after 73 min. Partial degradation of hydrogels were followed through decrease in their G' values. Total degradation was accepted as the inversion point of G' and G'' indicating the transition from viscoelastic solid into liquid like material. The degradation plot was obtained by calculating the percent loss in storage modulus and plotting it against time. From these curves, HG2k was observed to have the slowest degradation rate resulting in a complete degradation within 120 min (Figure 4.18) after addition of DTT. Degradation rate was observed to increase with the length of the crosslinker yielding a degradation period of 75 min (Figure 4.19) and 60 min (Figure 4.20) for HG6k and HG10k, respectively. Thus, HG2k hydrogels having the least porosity degraded last while HG10ks having the highest porosity degraded first, as expected. Importantly, hydrogels were stable up to 90% in acidic media (pH = 5.5) for more than an hour in the absence of DTT as deduced from the plateau during the first 73 min of

degradation plots. Due to the stability of hydrogels in acidic media, the reduction of disulfide bridges can be proposed as the main reaction responsible for degradation of hydrogels.

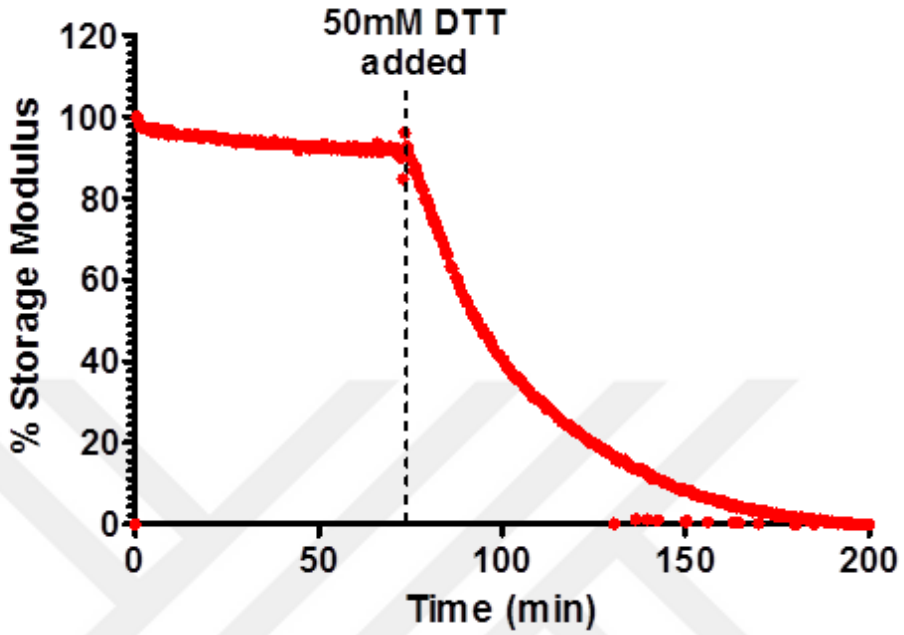

Figure 4.18. Degradation of HG2k followed by rheology.

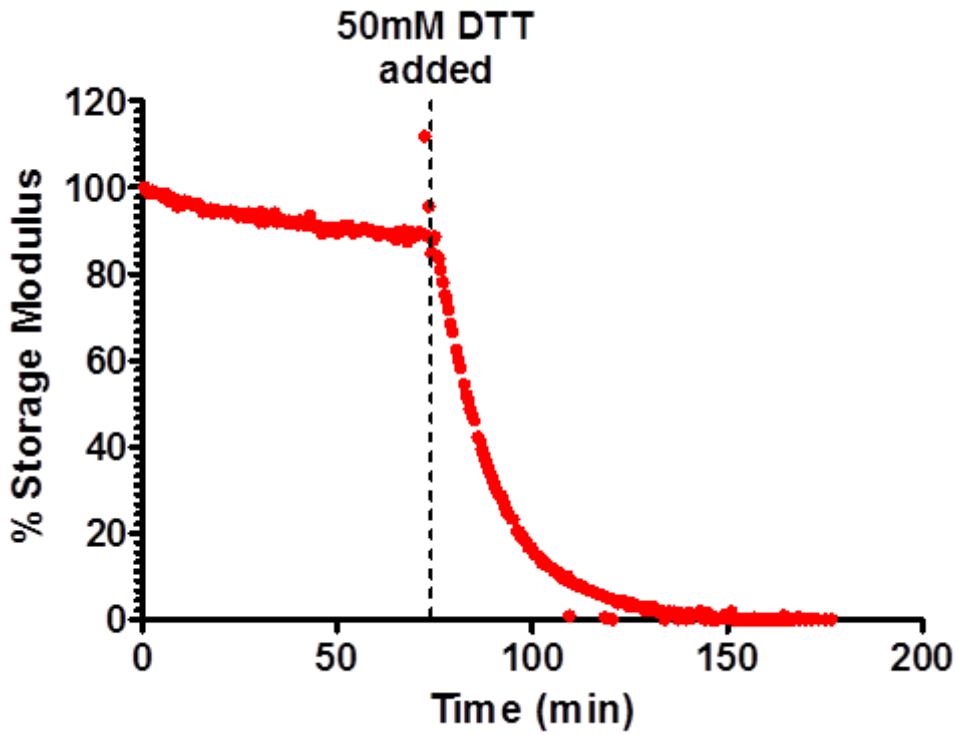

Figure 4.19. Degradation of HG6k followed by rheology.

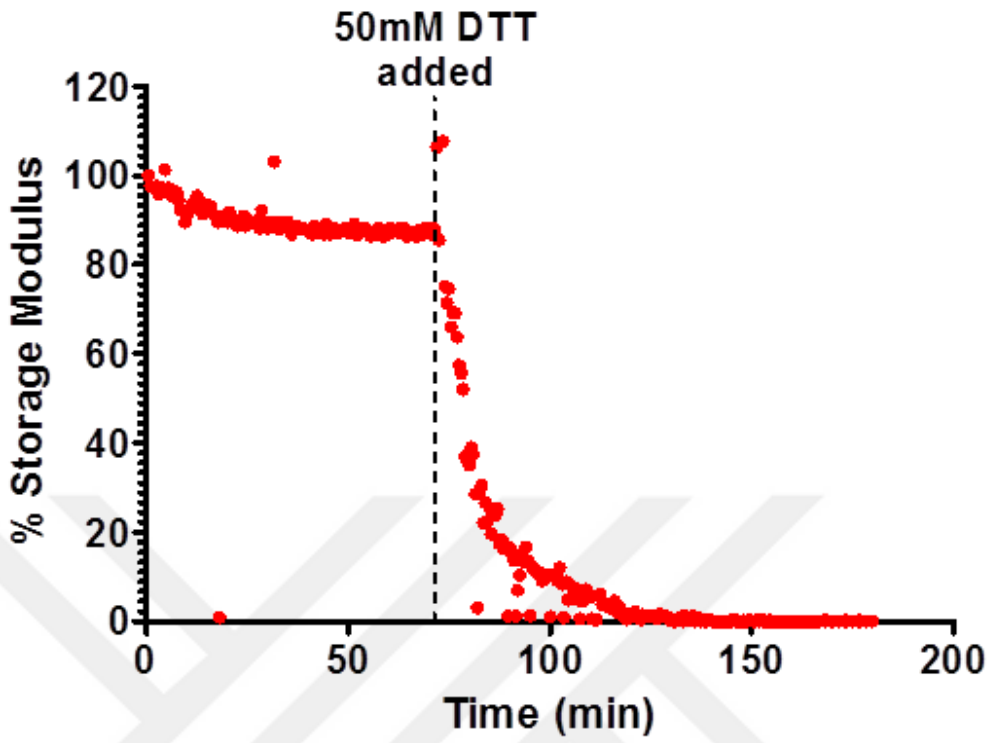

Figure 4.20. Degradation of HG10k followed by rheology.

4.5. Conjugation of Doxorubicin to Hydrogels

In order to prevent burst release of drug in biological environment and enhance the treatment period, DOX was attached to hydrogels through chemical bonding instead of physical encapsulation. Activated NHS groups on HG2k, HG6k and HG10k served as conjugation sites for the amine group on DOX. Since tumor environment is known to be slightly acidic and rich in glutathione with respect to healthy tissue [42], drug linkers were designed to be susceptible to those triggers. Thus, DOX conjugation strategy involved carbamate formation and redox-responsive disulfide bridges were introduced into drug linkers to obtain stimuli-responsive sustained release behavior (Figure 4.21).

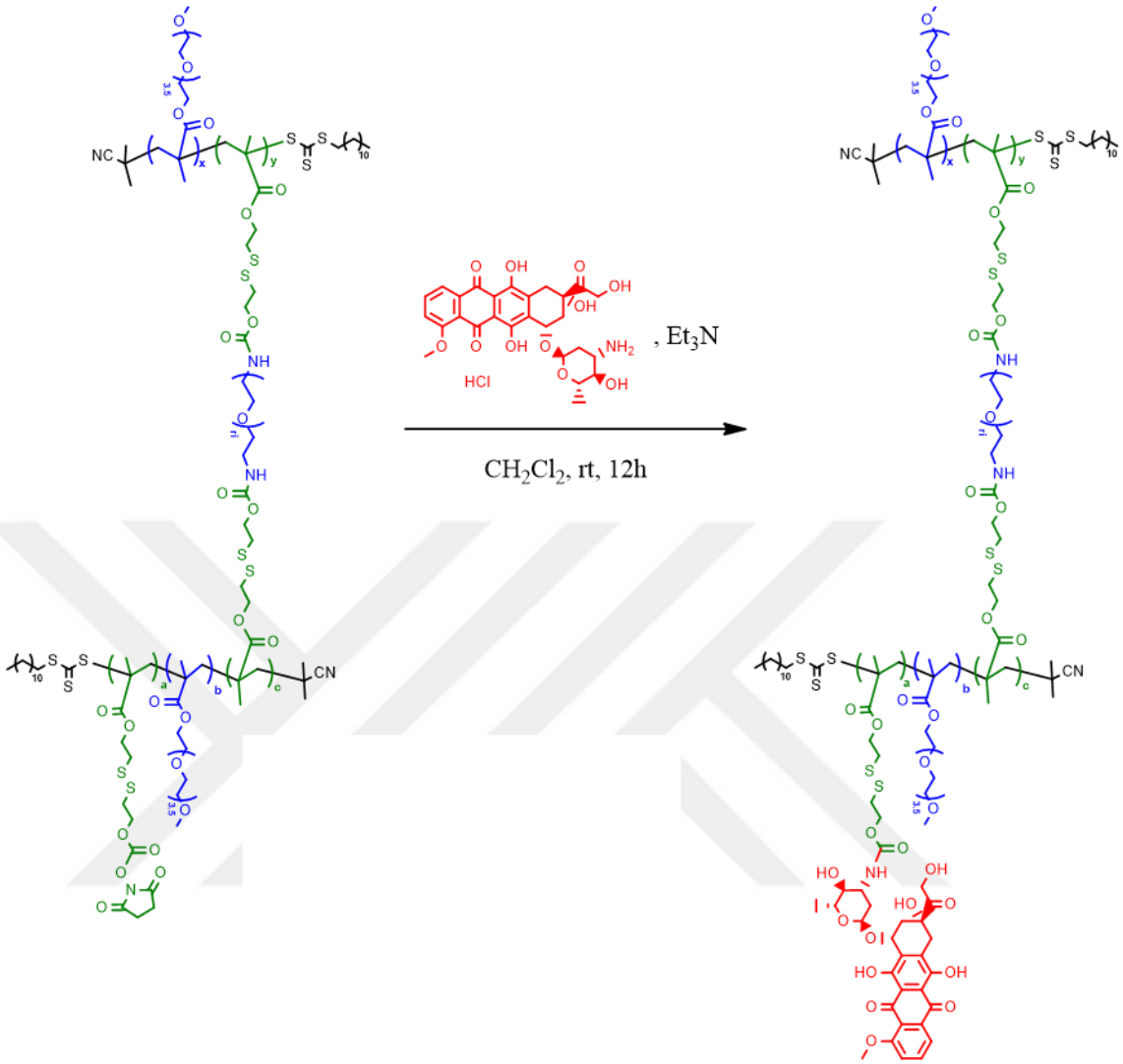

Figure 4.21. Chemical illustration of DOX conjugation to hydrogels.

Chemical conjugation of DOX was proven through FT-IR spectroscopy. C=O stretching at 1812 cm^{-1} and 1789 cm^{-1} which were coming from the NHS carbonyls were shown to disappear upon DOX conjugation (Figure 4.22). Although the functionalizable hydrogels were white in dry state, DOX conjugated hydrogels had bright red color characteristic of DOX. Photographic images of HG6k hydrogels before and after DOX conjugation are shown in Figure 4.23, as an example.

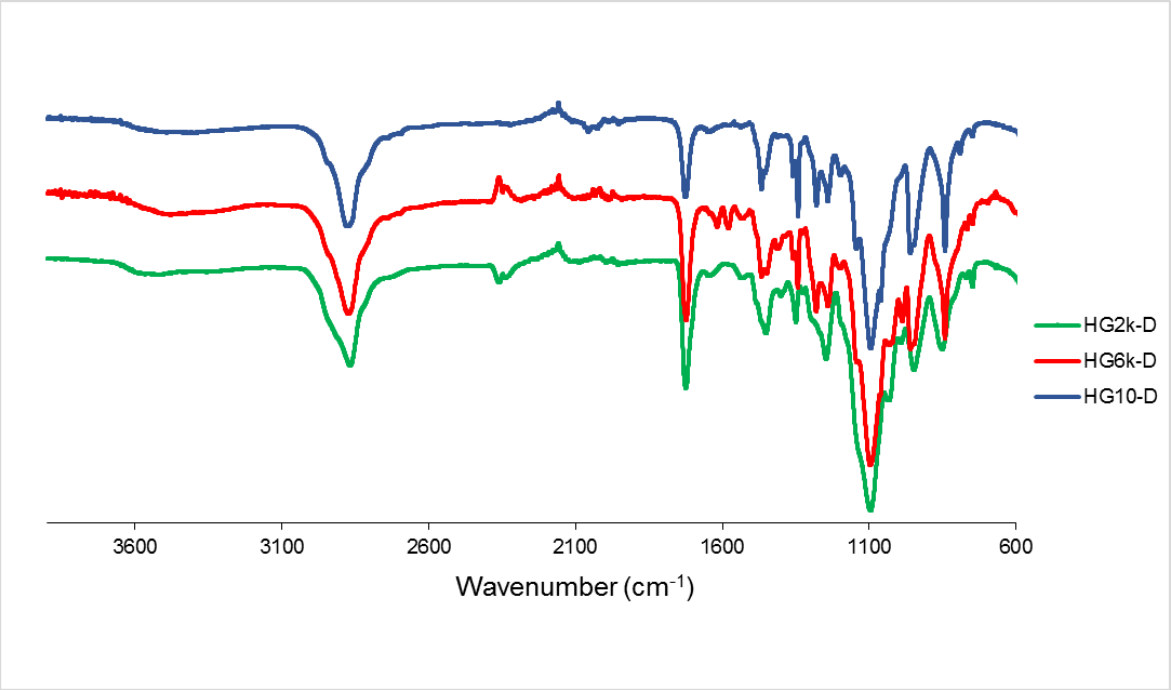

Figure 4.22. IR Spectra of DOX-conjugated hydrogels.

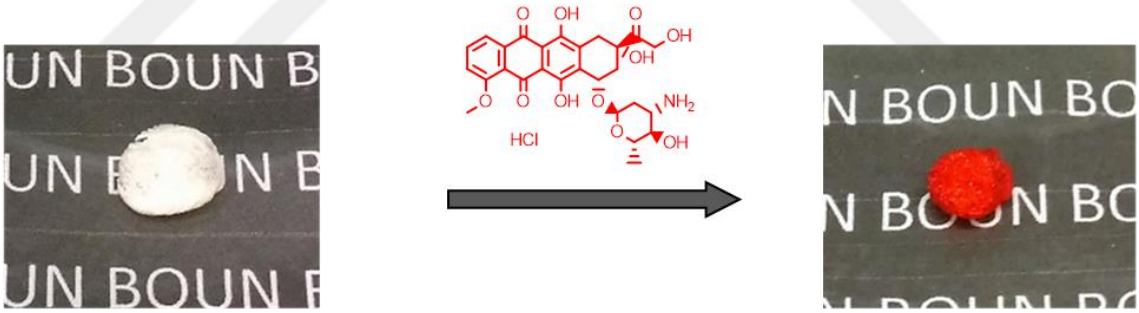

Figure 4.23. Photographic image of HG6k before and after DOX loading.

4.6. pH and Redox Triggered Release of Doxorubicin from Hydrogels

Tumor tissue is known to be slightly acidic and rich in GSH compared to healthy tissue as previously mentioned. Thus, a hydrogel construct releasing its cargo only in the presence of a tumor-based trigger is desired for smart drug delivery applications. In order to investigate pH and redox sensitive release behavior of hydrogels, DOX release was performed in 3 different conditions: physiological (PBS, pH = 7.4), acidic (NaOAc, pH = 5.5) and 5mM GSH bearing acidic condition.

To begin with, none of the hydrogels were expected to degrade and release their cargo under physiological conditions due to chemical conjugation of DOX and absence of an external trigger. This expectation was consistent with the low drug release from HG6k-D (Figure 4.25) and HG10k-D (Figure 4.26) at neutral pH but not HG2k-D (Figure 4.24). Although DOX release was lowest for HG2k-D at neural pH in the absence of a reducing environment, almost 40% of cumulative release was observed with large deviations. Considering that most of the drug is released within the first 10 h in PBS, this can be burst released drug which may have remained despite the extensive washing process before starting the experiment. Since HG2ks had the lowest porosity, it should be more difficult to get rid of the non-conjugated drug through washing compared to the others.

In addition, although cumulative release profiles were improved by acidic conditions for HG2k-D and HG10k-D, it was not enough for total release of cargo as the curve got stabilized around 60% for both hydrogels. This value was even less for for HG6k-D and was stabilized around 30%. It should also be mentioned that all 3 types of hydrogels remained intact on the course of the release experiments under both physiological and acidic conditions as expected from rheological analysis results. Thus, total release of the DOX content was not expected.

Importantly, cumulative DOX release was above 80% for all 3 types of hydrogels in a reducing environment. Thus, presence of a slightly reducing environment significantly improved release profiles of hydrogels. According to these results, we may conclude that DOX release was degradation dependent.

It is also worth to highlight that porosity of hydrogels had an impact on the release trends. For instance, the maximum DOX release was obtained around 9 days for HG2k-D while it was reached after 5 and 4 days for HG6k-D and HG10k-D, respectively. Thus, hydrogels with the lowest porosity degraded slower and released its content last and vice versa. In any case, burst release was prevented and DOX release was occurring in a sustained manner.

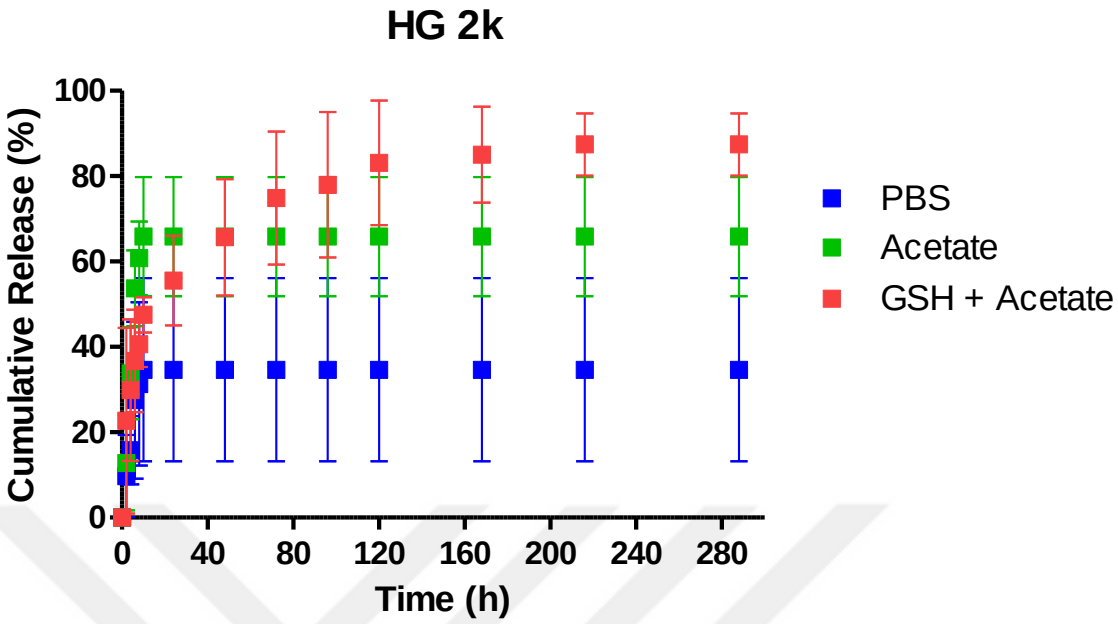

Figure 4.24. Release of DOX from HG2k.

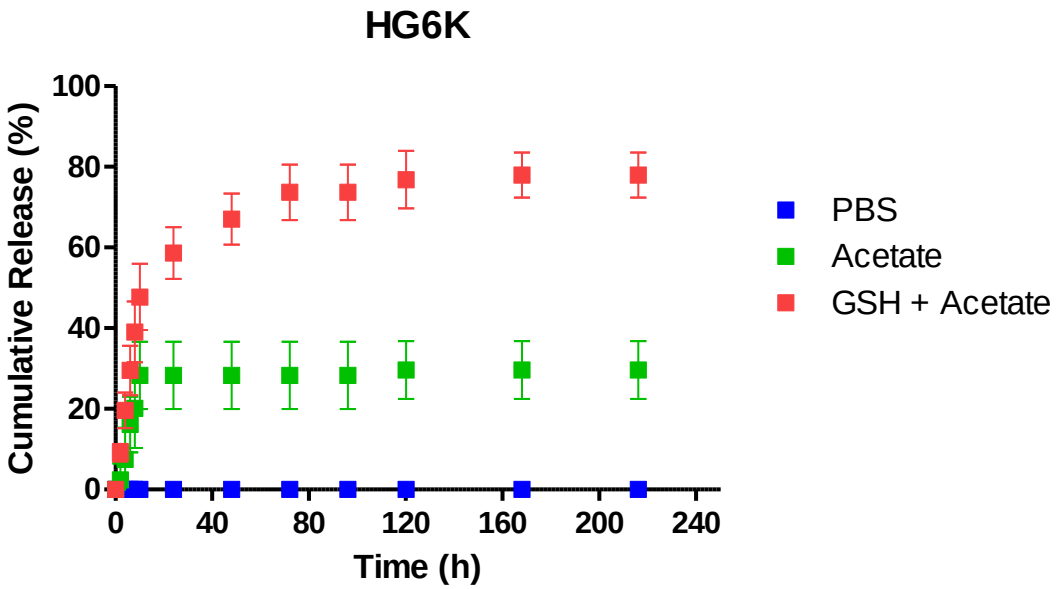

Figure 4.25. Release of DOX from HG6k

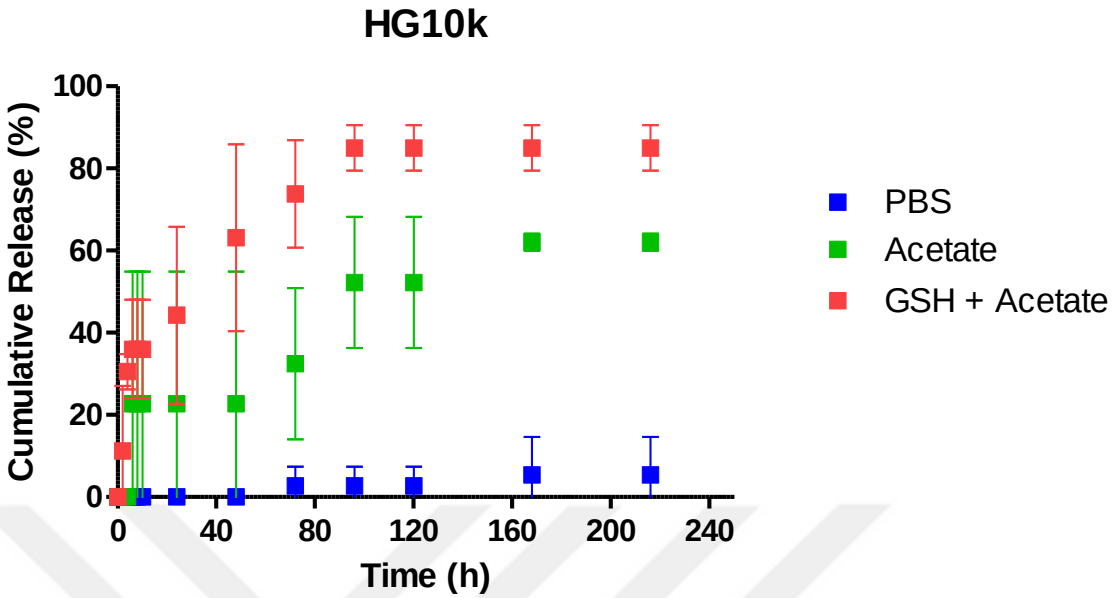

Figure 4.26. Release of DOX from HG10k.

5. CONCLUSIONS

In this thesis, pH and redox sensitive functionalizable hydrogels were obtained for local drug delivery of an anti-cancer drug, namely, DOX. For this purpose, a functionalizable polymer, poly(PEGMEMA-*co*-SCEDEMA) (M_n =12 kDa), with low PDI of 1.3 was synthesized via RAFT polymerization. Hydrogels were synthesized by crosslinking of poly(PEGMEMA-*co*-SCEDEMA) with PEG-diamine with different molecular weights. The length of the crosslinker was observed to affect the physical properties of hydrogels. Hydrogels with longest crosslinker had the lowest storage moduli and vice versa as deduced from rheological examination. Microstructure investigation showed that porosity was increasing with the molecular weight of the crosslinker. Consistently, hydrogels with the highest porosity degraded faster in the presence of a reducing environment such as DTT. Drug conjugation to the hydrogels was achieved by reacting the amine group of DOX with the activated-ester groups on hydrogels yielding carbamate at the conjugation site. Thus, a dual-stimuli responsive network was obtained for local drug delivery. For all 3 types of hydrogels, DOX release was observed to be pH and GSH dependent. Nevertheless, sustained release profiles extending up to 12 days were achieved for all types of hydrogels. Thus, these dual-stimuli responsive degradable hydrogels are promising for local drug delivery. Their therapeutic efficacy against tumor tissue needs to be further examined through *in vitro* studies.

REFERENCES

1. Peppas, N. A., P. Bures, W. Leobandung, and H. Ichikawa, "Hydrogels in pharmaceutical formulations", *European Journal of Pharmaceutics and* Biopharmaceutics, pp. 27-46, Vol. 50, 2000.
2. Hoffman, A. S., "Hydrogels for biomedical applications ", *Advanced Drug Delivery Reviews*, Vol. 64, pp. 18–23, 2012.
3. Caló, E. and V. V Khutoryanskiy, "Biomedical applications of hydrogels : A review of patents and commercial products", *European Polymer Journal*, Vol. 65, pp. 252–267, 2015.
4. Nuttelman, C. R., M. A. Rice, A. E. Rydholm, C. N. Salinas, N. Darshita, and K. S. Anseth, "Macromolecular Monomers for the Synthesis of Hydrogel Niches and Their Application in Cell Encapsulation and Tissue Engineering", *Progress in Polymer Science*, Vol. 33, No. 2, pp. 167–179, 2008.
5. Park, K. R. and Y. C. Nho, "Synthesis of PVA / PVP hydrogels having two-layer by radiation and their physical properties", *Radiation Physics and Chemistry*, Vol. 67, pp. 361–365, 2003.
6. Koetting, M. C., J. T. Peters, S. D. Steichen, and N. A. Peppas, "Stimulus-responsive hydrogels : Theory , modern advances , and applications", *Materials Science and Engineering R*, Vol. 93, pp. 1–49, 2015.
7. Krukiewicz, K. and J. K. Zak, "Biomaterial-based regional chemotherapy : Local anticancer drug delivery to enhance chemotherapy and minimize its side-effects", *Materials Science and Engineering C*, Vol. 62, pp. 927–942, 2016.
8. Singh, M. R., S. Patel, and D. Singh, *Chapter 9. Natural polymer-based hydrogels as scaffolds for tissue engineering*. Elsevier Inc., 2016.
9. Dong, H., C. Kil, Y. Sung, K. Hee, J. Hee, T. Hwang, T. Woo, and B. Cheol, "A chitosan hydrogel-based cancer drug delivery system exhibits synergistic antitumor effects by combining with a vaccinia viral vaccine", *International Journal of Pharmaceutics*, Vol. 350, pp. 27–34, 2008.
10. Aravamudhan, A., D. M. Ramos, A. A. Nada, and S. G. Kumbar, *Natural Polymers : Polysaccharides and Their Derivatives for Biomedical Applications*. Elsevier Inc., 2014.

11. Gibas, I. and H. Janik, "Review : Synthetic Polymer Hydrogels for Biomedical Applications", *Chemistry and Chemical Technology*, Vol. 4, No. 4, 2010.
12. Place, E. S., J. H. George, K. Williams, M. M. Stevens, "Synthetic polymer scaffolds for tissue engineering ", Chemical Society Reviews, Vol. 38, pp. 1139–1151, 2009.
13. Ercole, F., H. Thissen, K. Tsang, R. A. Evans, and J. S. Forsythe, "Photodegradable Hydrogels Made via RAFT", *Macromolecules, 45* (20), pp. 8387-8400, 2012.
14. Mespouille, L., L. Hedrick, and P. Dubois, "Expanding the role of chemistry to produce new amphiphilic polymer (co) networks", *Soft Matter*, Vol. 5, pp. 4878-4892 2009.
15. Tan, V. T. G., D. H. T. Nguyen, R. H. Utama, M. Kahram, F. Ercole, J. F. Quinn, M. R. Whittaker, T. P. Davis, and J. Justin Gooding, "Modular photo-induced RAFT polymerised hydrogels: Via thiol-ene click chemistry for 3D cell culturing", *Polymer Chemistry*, Vol. 8, No. 39, pp. 6123–6133, 2017.
16. Konieczynska, M. D. and M. W. Grinsta, "On-Demand Dissolution of Chemically Cross-Linked Hydrogels", *Accounts of Chemical Research*, Vol. 50, pp. 151−160, 2017.
17. Siegel, R. L. and K. D. Miller, "Cancer Statistics , 2019", *CA: A Cancer Journal for Clinicians*, Vol. 69, No. 1, pp. 7–34, 2019.
18. Sepantafar, M., R. Maheronnaghsh, H. Mohammadi, F. Radmanesh, M. M. Hasani-sadrabadi, and M. Ebrahimi, "Engineered Hydrogels in Cancer Therapy and Diagnosis", *Trends in Biotechnology*, Vol. 35, No. 11, pp. 1074–1087, 2017.
19. Knowlton, S., S. Onal, C. H. Yu, J. J. Zhao, and S. Tasoglu, "Bioprinting for cancer research", *Trends in Biotechnology.*, pp. 1–10, 2015.
20. Pradhan, S., J. M. Clary, D. Seliktar, and E. A. Lipke, "A three-dimensional spheroidal cancer model based on PEG-fibrinogen hydrogel microspheres", *Biomaterials*, Vol. 115, pp. 141–154, Jan. 2017.
21. Casey, J., X. Yue, T. D. Nguyen, A. Acun, V. R. Zellmer, S. Zhang, and P. Zorlutuna, "3D hydrogel-based microwell arrays as a tumor microenvironment model to study breast cancer growth", *Biomedical Materials*, Vol. 12, No. 2, 2017.
22. Duncan, R., K. Edward, and V. I. I. Avenue, "The Dawning Era Of Polymer Therapeutics", *Nature Reviews Drug Discovery*, Vol. 2, pp. 347–360, 2003.
23. Li, J. and D. J. Mooney, "Designing hydrogels for controlled drug delivery", *Nature Reviews Materials*, Vol. 1, pp. 1–18, 2016.

24. Wan, J., S. Geng, H. Zhao, X. Peng, Q. Zhou, H. Li, M. He, Y. Zhao, X. Yang, and H. Xu, "Doxorubicin-induced co-assembling nanomedicines with temperature-sensitive acidic polymer and their in-situ- forming hydrogels for intratumoral administration", *Journal of Controlled Release*, Vol. 235, pp. 328-336, 2016.
25. Nguyen, K., P. Ngoc, and E. Alsberg, "Acta Biomaterialia Functionalized , biodegradable hydrogels for control over sustained and localized siRNA delivery to incorporated and surrounding cells", *Acta Biomaterialia*, Vol. 9, No. 1, pp. 4487–4495, 2013.
26. Li, L., J. Gu, J. Zhang, Z. Xie, Y. Lu, L. Shen, Q. Dong, and Y. Wang, "Injectable and Biodegradable pH-Responsive Hydrogels for Localized and Sustained Treatment of Human Fibrosarcoma", *ACS Applied Materials and Interfaces*, Vol. 7, pp. 1944-8244, 2015.
27. Aydin, D., M. Arslan, A. Sanyal, and R. Sanyal, "Hooked on Cryogels: A Carbamate Linker Based Depot for Slow Drug Release", *Bioconjugate Conjugate*, Vol. 28, pp. 1443−1451, 2017.
28. Peppas, B. N. A., J. Z. Hilt, A. Khademhosseini, and R. Langer, "Hydrogels in Biology and Medicine : From Molecular Principles to Bionanotechnology", *Advanced Materials*, Vol. 18, pp. 1345–1360, 2006.
29. Rizwan, M., R. Yahya, A. Hassan, M. Yar, A. D. Azzahari, V. Selvanathan, F. Sonsudin, and C. N. Abouloula, "pH sensitive hydrogels in drug delivery: Brief history, properties, swelling, and release mechanism, material selection and applications", *Polymers (Basel).*, Vol. 9, No. 4, 2017.
30. Qiu, Y. and K. Park, "Environment-sensitive hydrogels for drug delivery", *Advanced Drug Delivery Reviews*, Vol. 64, pp. 49–60, 2012.
31. Knipe, J. M. and N. A. Peppas, "Multi-responsive hydrogels for drug delivery and tissue engineering applications", *Regenerative Biomaterials*, Vol. 1, pp. 57–65, 2014.
32. Ghavaminejad, A., M. Samarikhalaj, L. E. Aguilar, C. H. Park, and C. S. Kim, "pH / NIR Light-Controlled Multidrug Release via a Mussel-Inspired Nanocomposite Hydrogel for Chemo-Photothermal Cancer Therapy", *Scientific Reports*, Vol. 6, pp. 1–12, 2016.
33. Hu, J., Y. Chen, Y. Li, Z. Zhou, and Y. Cheng, "Biomaterials A thermo-degradable hydrogel with light-tunable degradation and drug release", *Biomaterials*, Vol. 112, pp. 133–140, 2017.

34. Kumar, V., J. Kim, S. Son, W. Jong, M. A. Repka, and S. Jo, "Acta Biomaterialia Matrix metalloproteinase-sensitive thermogelling polymer for bioresponsive local drug delivery", *Acta Biomaterialia*, Vol. 7, No. 5, pp. 1984–1992, 2011.
35. Huebsch, N., C. J. Kearney, X. Zhao, J. Kim, C. A. Cezar, and Z. Suo, "Ultrasound-triggered disruption and self-healing of reversibly cross-linked hydrogels for drug delivery and enhanced chemotherapy", *Proceedings of the National Academy of Sciences of the United States of America*, Vol. 111, pp. 9762-7, 2014.
36. He, M., J. Sui, Y. Chen, S. Bian, and Y. Cui, " Localized multidrug co-delivery by injectable self-crosslinking hydrogel for synergistic combinational chemotherapy", *Journal of Materials Chemistry B*, pp. 4852–4862, 2017.
37. Pramudya, I., C. Kim, and H. Chung, "Synthesis and adhesion control of glucose-based bioadhesive: Via strain-promoted azide-alkyne cycloaddition", *Polymer Chemistry*, Vol. 9, No. 26, pp. 3638–3650, 2018.
38. Fairbanks, B. D., P. A. Gunatillake, and L. Meagher, "Biomedical applications of polymers derived by reversible addition - fragmentation chain-transfer (RAFT)", *Advanced Drug Delivery Reviews*, Vol. 91, pp. 141–152, 2015.
39. Ghosh, A. K. and M. Brindisi, "Organic Carbamates in Drug Design and Medicinal Chemistry", *Journal of Medicinal Chemistry*, Vol. 58, No. 7, pp. 2895–2940, 2015.
40. Zuidema, J. M., C. J. Rivet, R. J. Gilbert, and F. A. Morrison, "A protocol for rheological characterization of hydrogels for tissue engineering strategies", *Journal of Biomedical Materials Research - Part B Applied Biomaterials*, Vol. 102, No. 5, pp. 1063–1073, 2014.
41. Spectus, C. O. N., "Soluble Polymer Carriers for the Treatment of Cancer : The Importance of Molecular Architecture", *Accounts of Chemical Research*, Vol. 42, No. 8, pp. 1141–1151, 2009.
42. Schmaljohann, D., "Thermo- and pH-responsive polymers in drug delivery", *Advanced Drug Delivery Reviews*, Vol. 58, pp. 1655–1670, 2006.
43. Karaçivi, M., "*Smart Polymeric Carriers: Targeted Delivery of Therapeutic Agents"*, PhD, Bogazici University, 2019.

APPENDIX A: ADDITIONAL DATA

IR spectra of poly(PEGMEMA-*co*-SCEDEMA), HG2k and HG10 hydrogels before and after 1-amino-2-propanol treatment and full GPC plot of poly(PEGMEMA-*co*-SCEDEMA are represented as additional data.

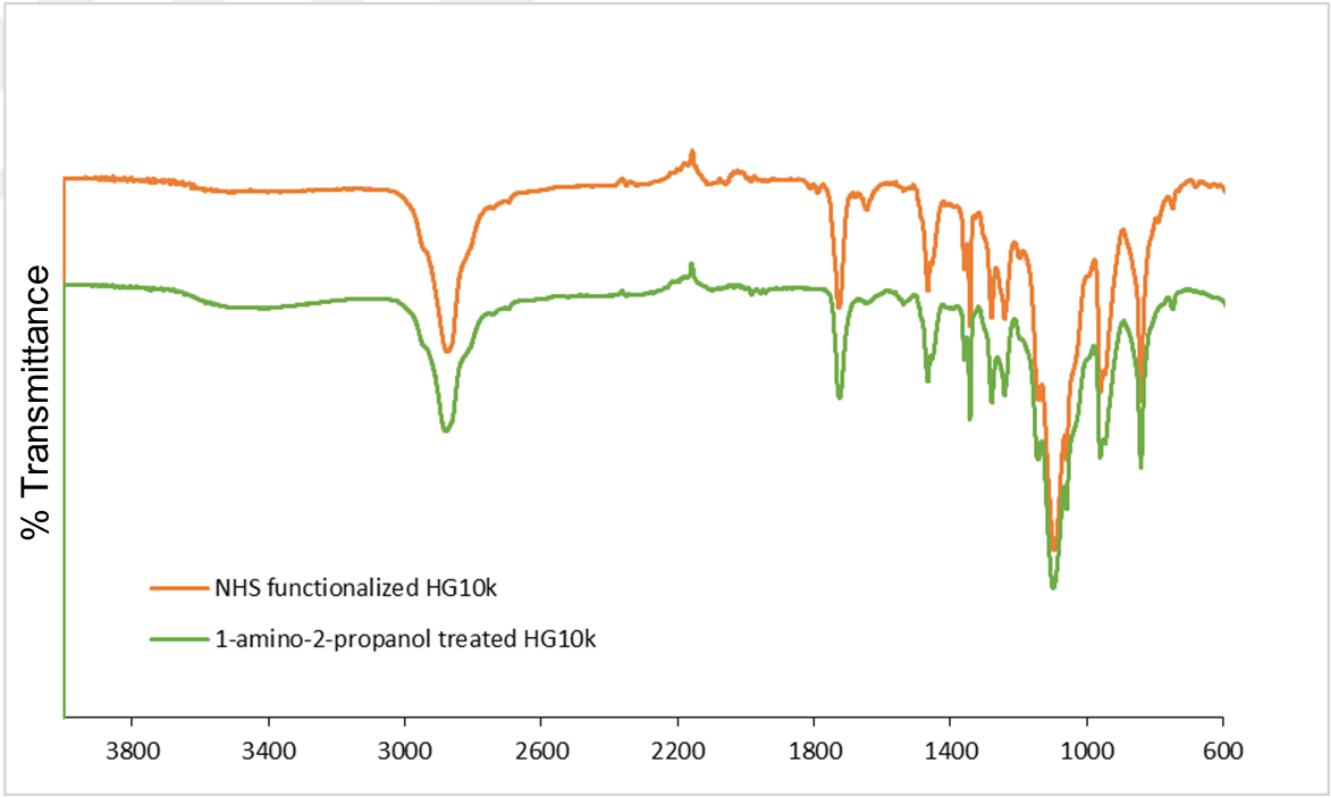

Figure A.1. FT-IR Spectra of NHS functionalized and 1-amino-2-propanol treated HG10k.

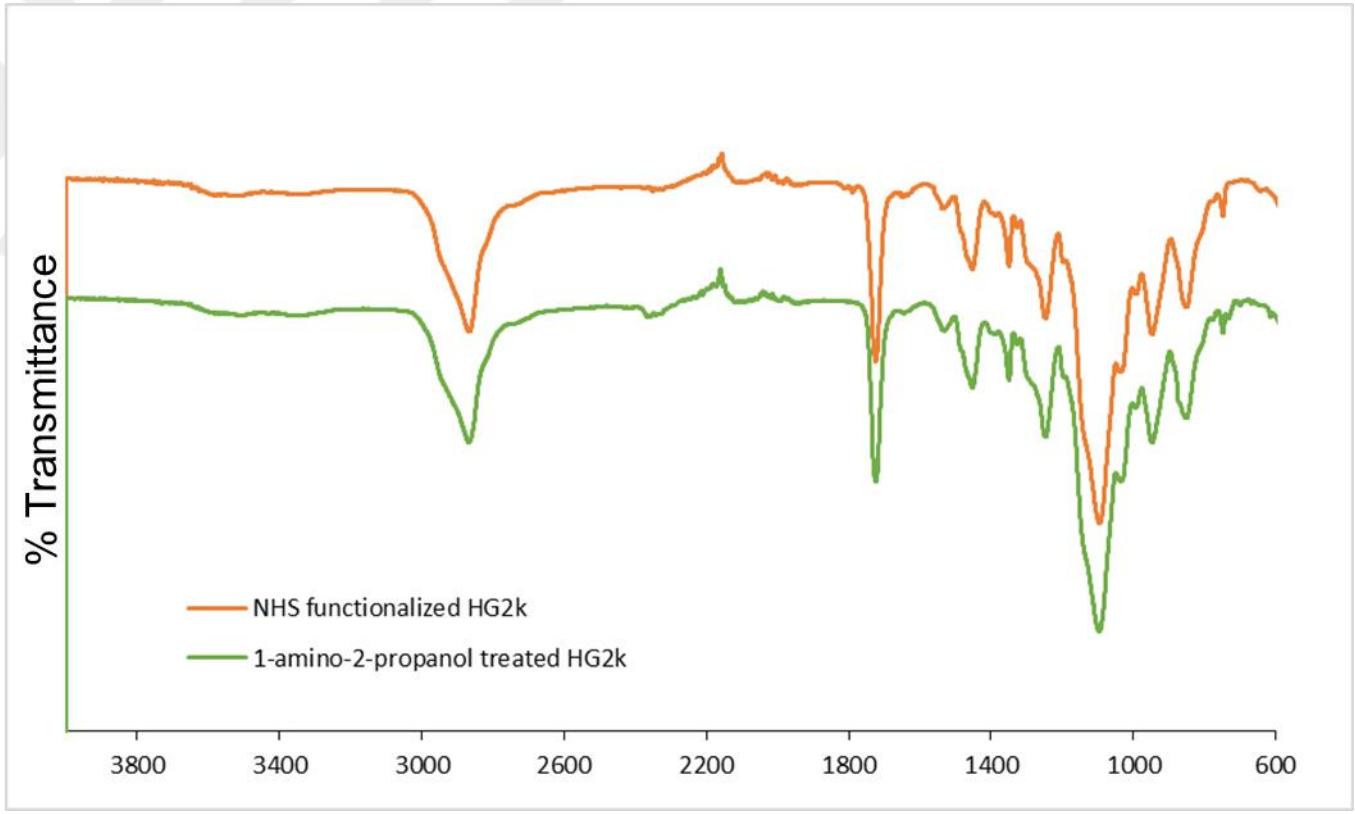

Figure A.2. Figure A.1. FT-IR Spectra of NHS functionalized and 1-amino-2-propanol treated HG2k.

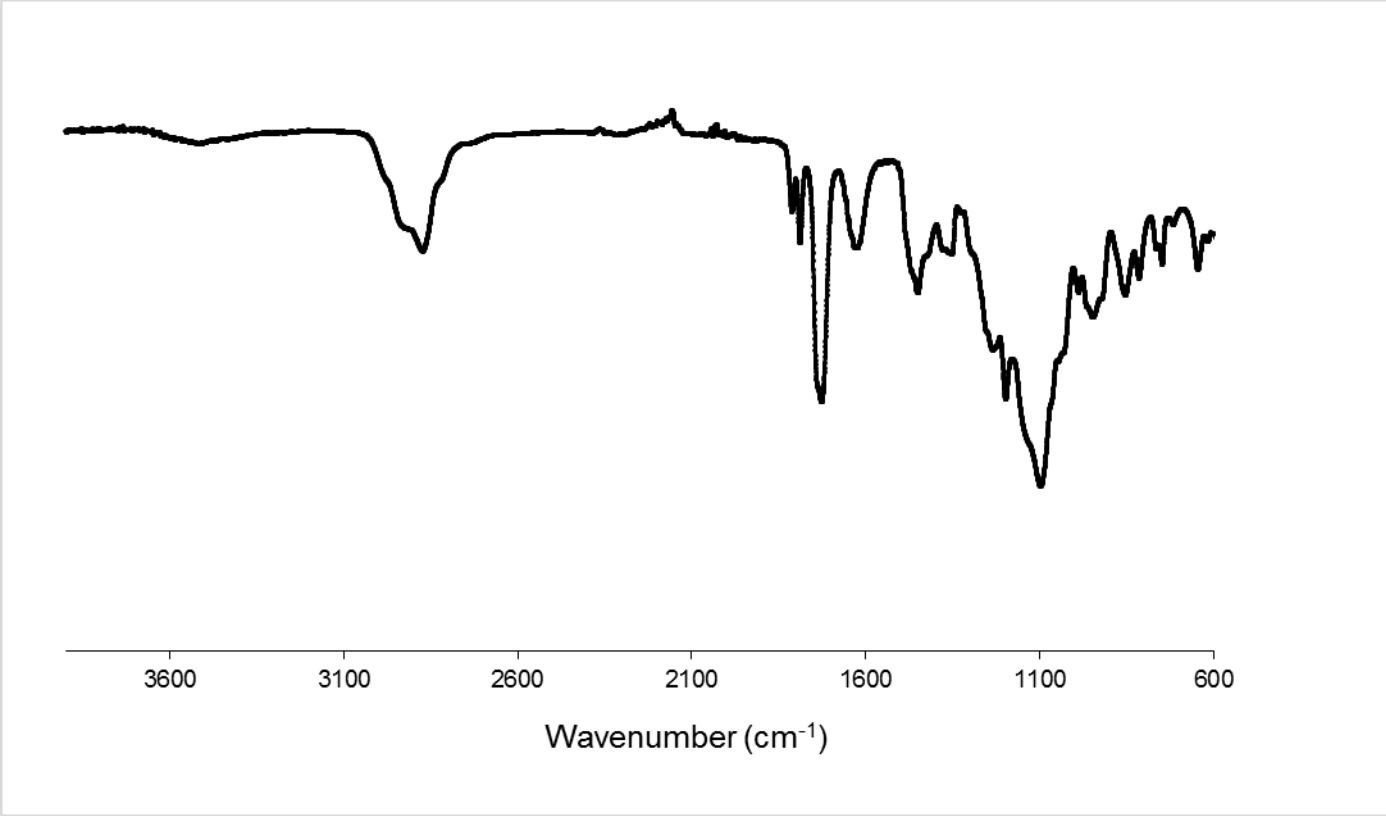

Figure A.3. FT-IR Spectrum of poly(PEGMEMA-*co*-SCEDEMA).

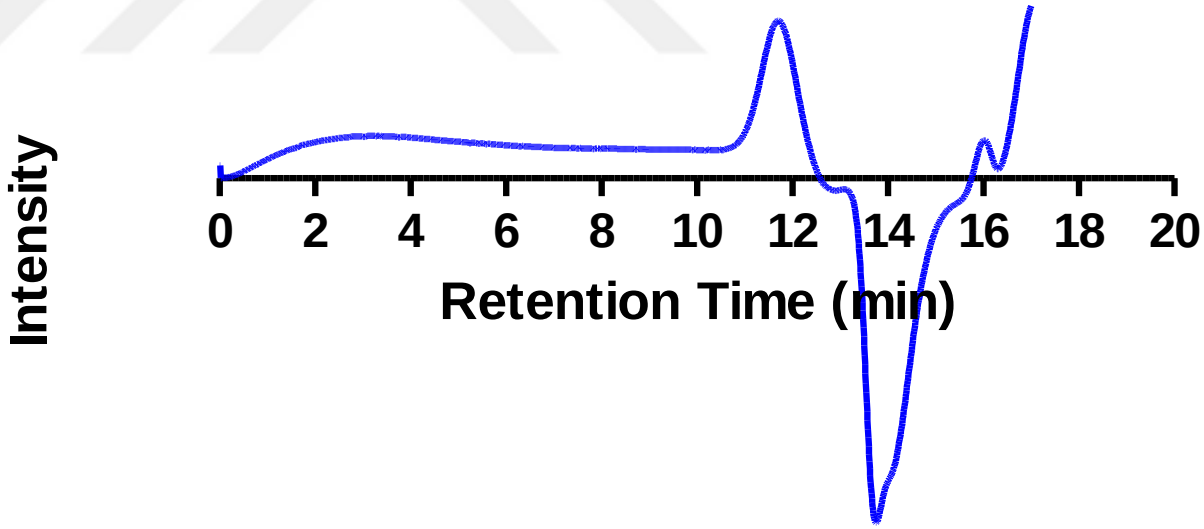

Figure A.4. Full GPC plot of poly(PEGMEMA-*co*-SCEDEMA.

APPENDIX B: COPYRIGHT NOTICES

Copyright notices for the figures utilized in this thesis are represented in this section.

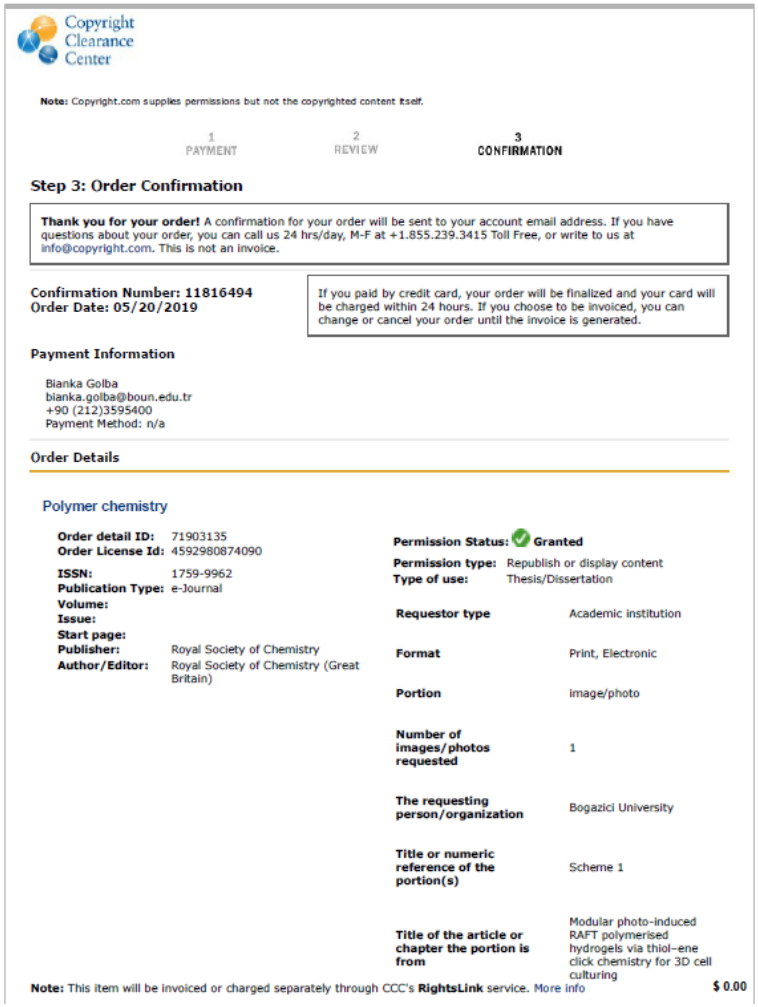

Copyright Clearance Center

Note: Copyright.com supplies permissions but not the copyrighted content itself.

1 PAYMENT 2 REVIEW 3 CONFIRMATION

Step 3: Order Confirmation

Thank you for your order! A confirmation for your order will be sent to your account email address. If you have questions about your order, you can call us 24 hrs/day, M-F at +1.855.239.3415 Toll Free, or write to us at info@copyright.com. This is not an invoice.

Confirmation Number: 11816494
Order Date: 05/20/2019

If you paid by credit card, your order will be finalized and your card will be charged within 24 hours. If you choose to be invoiced, you can change or cancel your order until the invoice is generated.

Payment Information

Bianka Golba
bianka.golba@boun.edu.tr
+90 (212)3595400
Payment Method: n/a

Order Details

Polymer chemistry

Order detail ID:	71903135
Order License Id:	4592980874090
ISSN:	1759-9962
Publication Type:	e-Journal
Volume:	
Issue:	
Start page:	
Publisher:	Royal Society of Chemistry
Author/Editor:	Royal Society of Chemistry (Great Britain)

Permission Status:	**Granted**
Permission type:	Republish or display content
Type of use:	Thesis/Dissertation
Requestor type	Academic institution
Format	Print, Electronic
Portion	image/photo
Number of images/photos requested	1
The requesting person/organization	Bogazici University
Title or numeric reference of the portion(s)	Scheme 1
Title of the article or chapter the portion is from	Modular photo-induced RAFT polymerised hydrogels via thiol–ene click chemistry for 3D cell culturing

Note: This item will be invoiced or charged separately through CCC's **RightsLink** service. More info **$ 0.00**

Figure B.1. Copyright notice for Figure 1.2.

ELSEVIER LICENSE
TERMS AND CONDITIONS

May 20, 2019

This Agreement between Ms. Bianka Golba ("You") and Elsevier ("Elsevier") consists of your license details and the terms and conditions provided by Elsevier and Copyright Clearance Center.

License Number	4592990691364
License date	May 20, 2019
Licensed Content Publisher	Elsevier
Licensed Content Publication	Trends in Biotechnology
Licensed Content Title	Engineered Hydrogels in Cancer Therapy and Diagnosis
Licensed Content Author	Mohammadmajid Sepantafar,Reihan Maheronnaghsh,Hossein Mohammadi,Fatemeh Radmanesh,Mohammad Mahdi Hasani-sadrabadi,Marzieh Ebrahimi,Hossein Baharvand
Licensed Content Date	Nov 1, 2017
Licensed Content Volume	35
Licensed Content Issue	11
Licensed Content Pages	14
Start Page	1074
End Page	1087
Type of Use	reuse in a thesis/dissertation
Intended publisher of new work	other
Portion	figures/tables/illustrations
Number of figures/tables /illustrations	1
Format	both print and electronic
Are you the author of this Elsevier article?	No
Will you be translating?	No
Original figure numbers	Figure 3
Title of your thesis/dissertation	Degradable Hydrogels For Local Drug Delivery
Publisher of new work	Bogazici University
Expected completion date	Jun 2019
Estimated size (number of pages)	1
Requestor Location	Ms. Bianka Golba Bogazici University, Bebek Mh., 34342 Beşiktaş/İstanbul Istanbul, Bebek 34342 Turkey

Figure B.2. Copyright notice for Figure 1.3.

SPRINGER NATURE LICENSE
TERMS AND CONDITIONS

May 20, 2019

This Agreement between Ms. Bianka Golba ("You") and Springer Nature ("Springer Nature") consists of your license details and the terms and conditions provided by Springer Nature and Copyright Clearance Center.

License Number	4592980003501
License date	May 20, 2019
Licensed Content Publisher	Springer Nature
Licensed Content Publication	Nature Reviews Materials
Licensed Content Title	Designing hydrogels for controlled drug delivery
Licensed Content Author	Jianyu Li, David J. Mooney
Licensed Content Date	Oct 18, 2016
Licensed Content Volume	1
Licensed Content Issue	12
Type of Use	Thesis/Dissertation
Requestor type	academic/university or research institute
Format	print and electronic
Portion	figures/tables/illustrations
Number of figures/tables /illustrations	2
High-res required	no
Will you be translating?	no
Circulation/distribution	<501
Author of this Springer Nature content	no
Title	Degradable Hydrogels For Local Drug Delivery
Institution name	Bogazici University
Expected presentation date	Jun 2019
Portions	Figure 3 and Figure 4
Requestor Location	Ms. Bianka Golba Bogazici University, Bebek Mh., 34342 Beşiktaş/İstanbul Istanbul, Bebek 34342 Turkey Attn: Ms. Bianka Golba
Total	0.00 USD

Figure B.3. Copyright notice for Figure 1.4 and Figure 1.5.

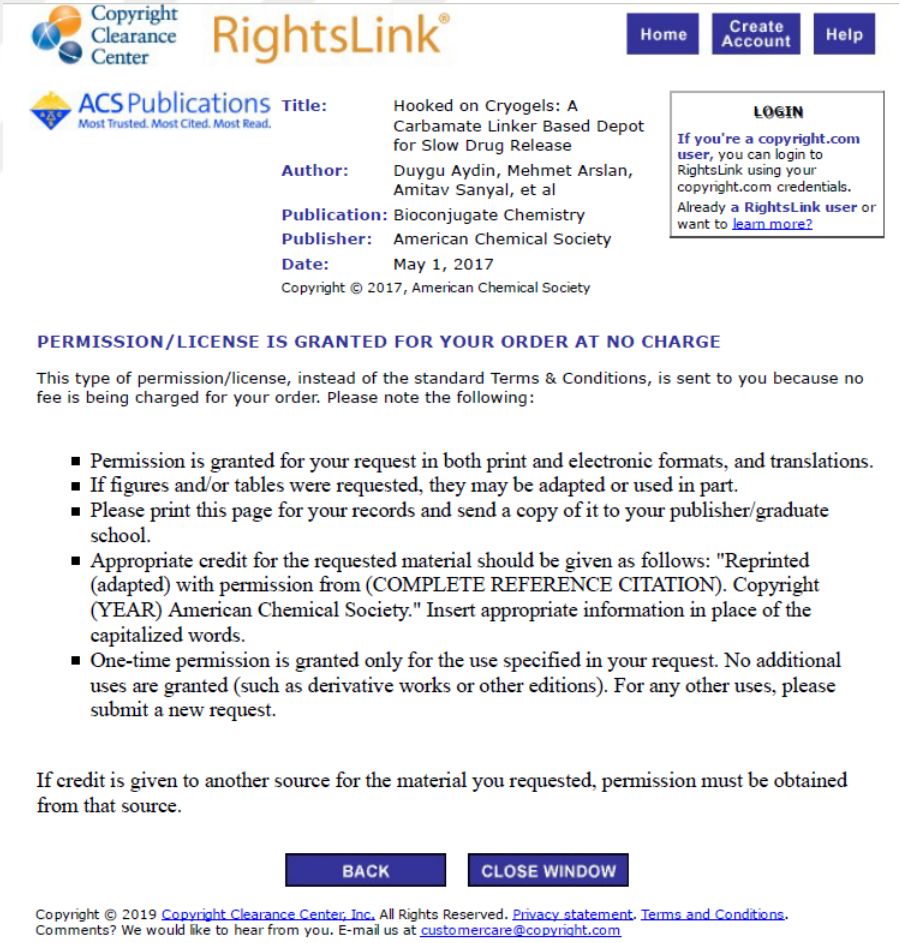

Copyright Clearance Center RightsLink®

Home | Create Account | Help

ACS Publications
Most Trusted. Most Cited. Most Read.

Title: Hooked on Cryogels: A Carbamate Linker Based Depot for Slow Drug Release

Author: Duygu Aydin, Mehmet Arslan, Amitav Sanyal, et al

Publication: Bioconjugate Chemistry

Publisher: American Chemical Society

Date: May 1, 2017

Copyright © 2017, American Chemical Society

LOGIN

If you're a copyright.com user, you can login to RightsLink using your copyright.com credentials.

Already a RightsLink user or want to learn more?

PERMISSION/LICENSE IS GRANTED FOR YOUR ORDER AT NO CHARGE

This type of permission/license, instead of the standard Terms & Conditions, is sent to you because no fee is being charged for your order. Please note the following:

- Permission is granted for your request in both print and electronic formats, and translations.
- If figures and/or tables were requested, they may be adapted or used in part.
- Please print this page for your records and send a copy of it to your publisher/graduate school.
- Appropriate credit for the requested material should be given as follows: "Reprinted (adapted) with permission from (COMPLETE REFERENCE CITATION). Copyright (YEAR) American Chemical Society." Insert appropriate information in place of the capitalized words.
- One-time permission is granted only for the use specified in your request. No additional uses are granted (such as derivative works or other editions). For any other uses, please submit a new request.

If credit is given to another source for the material you requested, permission must be obtained from that source.

BACK | CLOSE WINDOW

Copyright © 2019 Copyright Clearance Center, Inc. All Rights Reserved. Privacy statement. Terms and Conditions.
Comments? We would like to hear from you. E-mail us at customercare@copyright.com

Figure B.4. Copyright notice for Figure 1.6.

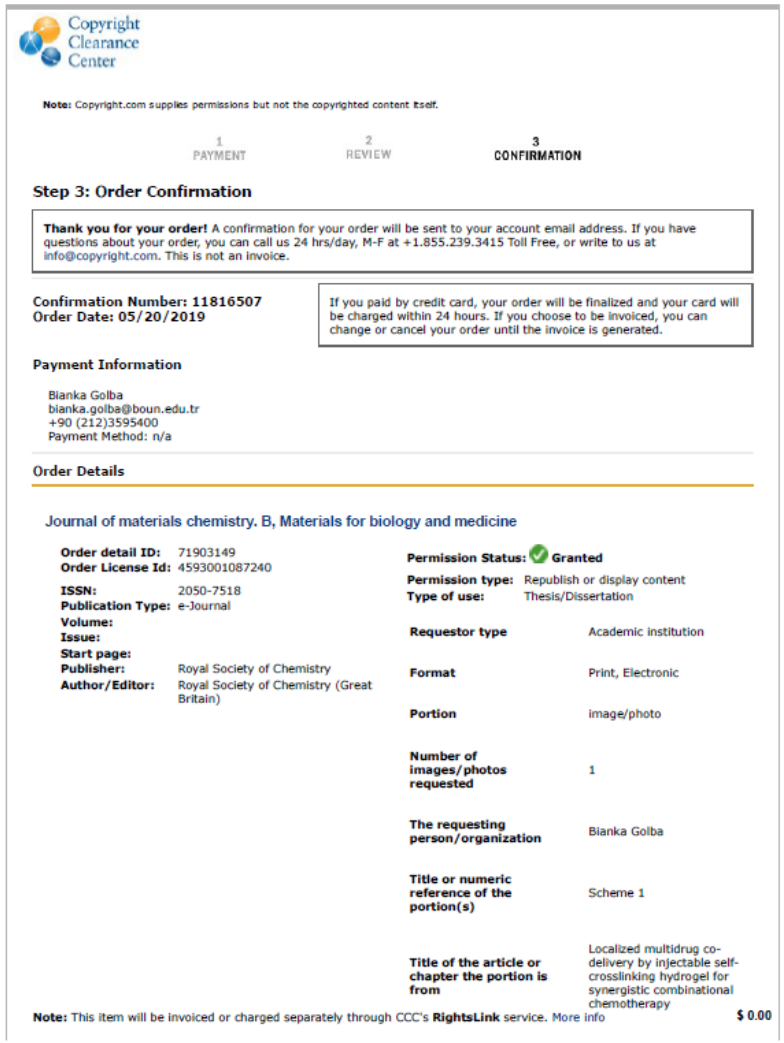

Copyright Clearance Center

Note: Copyright.com supplies permissions but not the copyrighted content itself.

1 PAYMENT 2 REVIEW 3 CONFIRMATION

Step 3: Order Confirmation

Thank you for your order! A confirmation for your order will be sent to your account email address. If you have questions about your order, you can call us 24 hrs/day, M-F at +1.855.239.3415 Toll Free, or write to us at info@copyright.com. This is not an invoice.

Confirmation Number: 11816507
Order Date: 05/20/2019

If you paid by credit card, your order will be finalized and your card will be charged within 24 hours. If you choose to be invoiced, you can change or cancel your order until the invoice is generated.

Payment Information

Bianka Golba
bianka.golba@boun.edu.tr
+90 (212)3595400
Payment Method: n/a

Order Details

Journal of materials chemistry. B, Materials for biology and medicine

Order detail ID:	71903149
Order License Id:	4593001087240
ISSN:	2050-7518
Publication Type:	e-Journal
Volume:	
Issue:	
Start page:	
Publisher:	Royal Society of Chemistry
Author/Editor:	Royal Society of Chemistry (Great Britain)

Permission Status:	**Granted**
Permission type:	Republish or display content
Type of use:	Thesis/Dissertation
Requestor type	Academic institution
Format	Print, Electronic
Portion	image/photo
Number of images/photos requested	1
The requesting person/organization	Bianka Golba
Title or numeric reference of the portion(s)	Scheme 1
Title of the article or chapter the portion is from	Localized multidrug co-delivery by injectable self-crosslinking hydrogel for synergistic combinational chemotherapy

Note: This item will be invoiced or charged separately through CCC's **RightsLink** service. More info **$ 0.00**

Figure B.5. Copyright notice for Figure 1.8.